

Cosmic-Rays in Galactic Winds and Outflows

Gwenael Giacinti (MPIK Heidelberg)

&

Andrew M. Taylor (DIAS, Dublin)

Taylor & Giacinti, submitted to Phys. Rev. D

+ In preparation

Outline

I – GALACTOCENTRIC OUTFLOW → *Fermi bubbles?*, GALACTIC CENTRE «PEVATRON»

II – GALACTIC WINDS → *Hardening,...? 200GV break?*

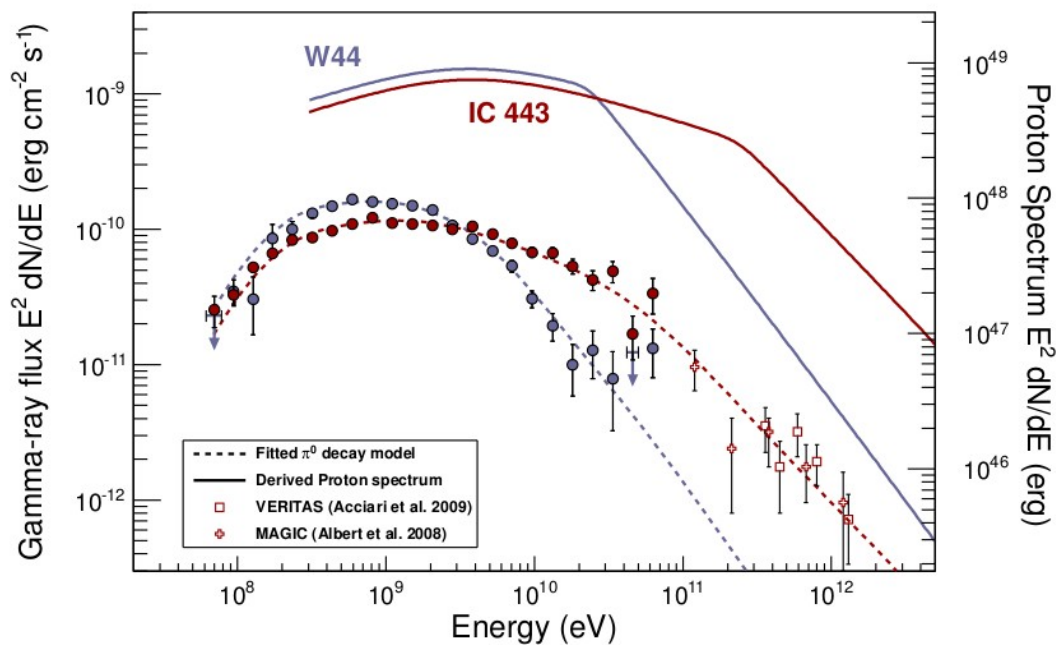
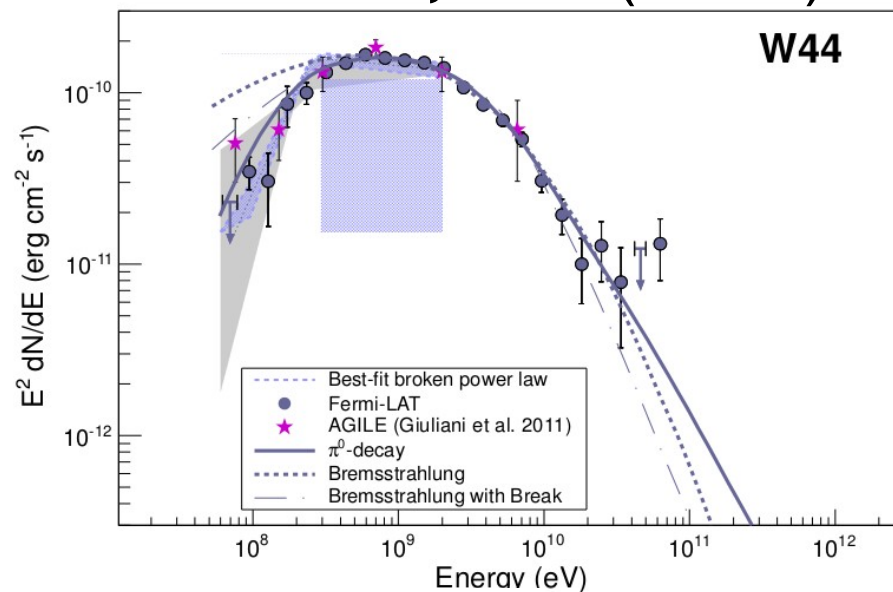
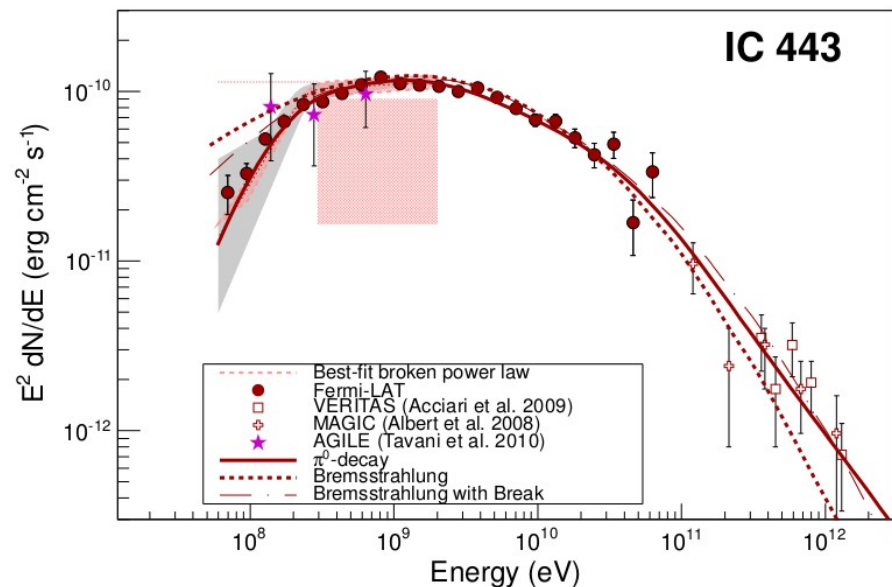
III - CR ANISOTROPY AS A PROBE OF LOCAL CR TRANSPORT PROPERTIES → *New probe !*

**I – GALACTOCENTRIC OUTFLOW,
GALACTIC CENTRE « PEVATRON »**

Taylor & Giacinti, arXiv:1607.08862

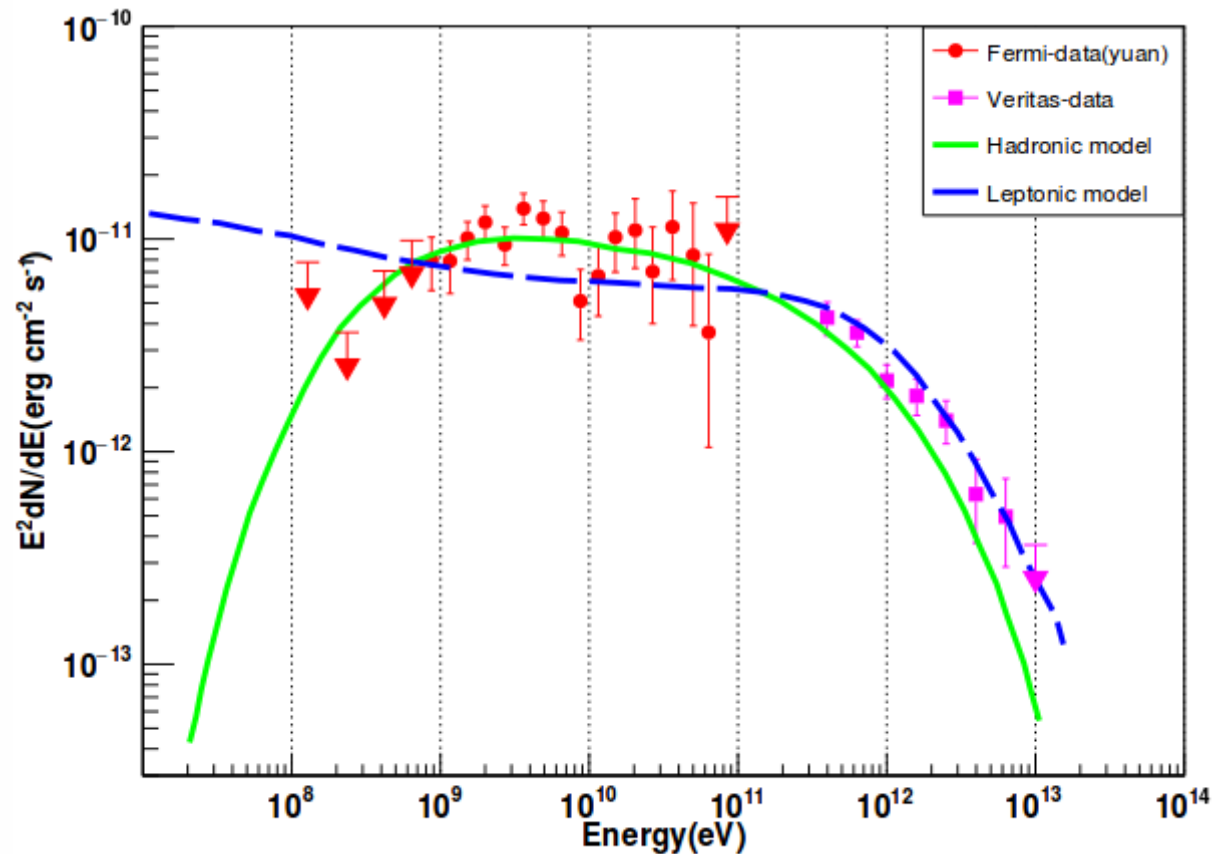
In γ – rays :

→ Old SNRs : Fermi-LAT coll., Science **339**, 807 (2013)



In γ – rays :

→ Historical SNRs : Particles up to ~ 100 's TeV only !

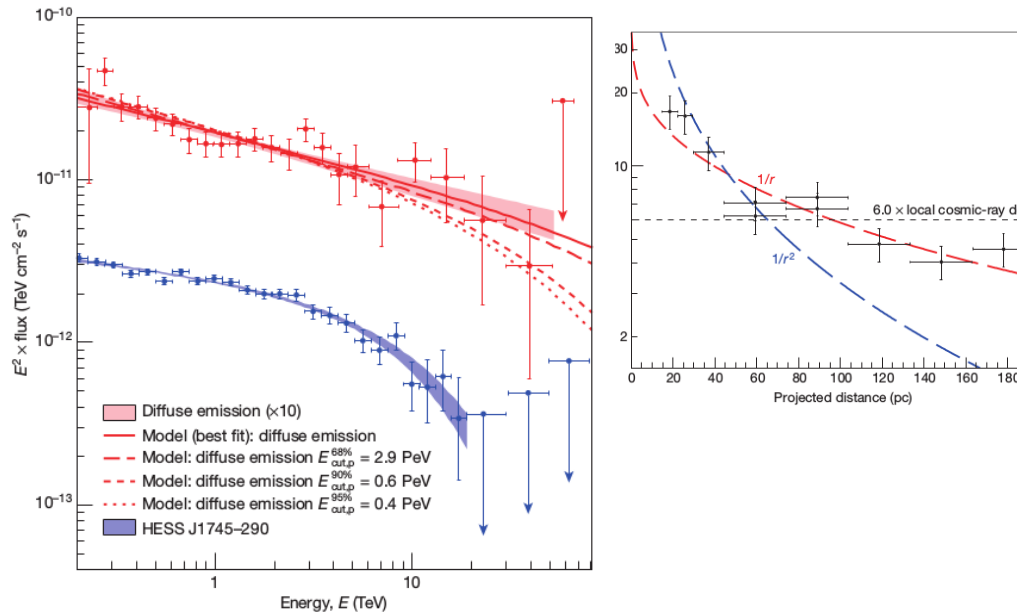


(Cas A, VERITAS, 1609.02881)

... **So where are the PeVatrons ?**

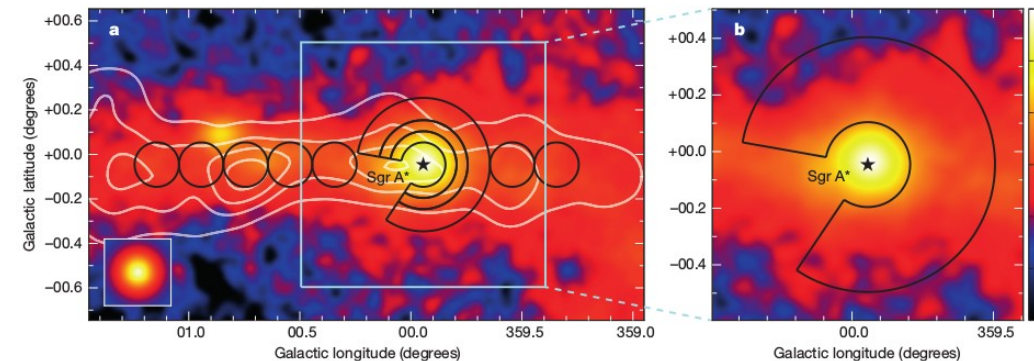
Acceleration of petaelectronvolt protons in the Galactic Centre

HESS Collaboration*



Galactic cosmic rays reach energies of at least a few petaelectronvolts¹ (of the order of 10^{15} electronvolts). This implies that our Galaxy contains petaelectronvolt accelerators ('PeVatrons'), but all proposed models of Galactic cosmic-ray accelerators encounter difficulties at exactly these energies². Dozens of Galactic accelerators capable of accelerating particles to energies of tens of teraelectronvolts (of the order of 10^{13} electronvolts) were inferred from recent γ -ray observations³. However, none of the currently known accelerators—not even the handful of shell-type supernova remnants commonly believed to supply most Galactic cosmic rays—has shown the characteristic tracers of petaelectronvolt particles, namely, power-law spectra of γ -rays extending without a cut-off or a spectral break to tens of teraelectronvolts⁴. Here we report deep γ -ray observations with arcminute angular resolution of the region surrounding the

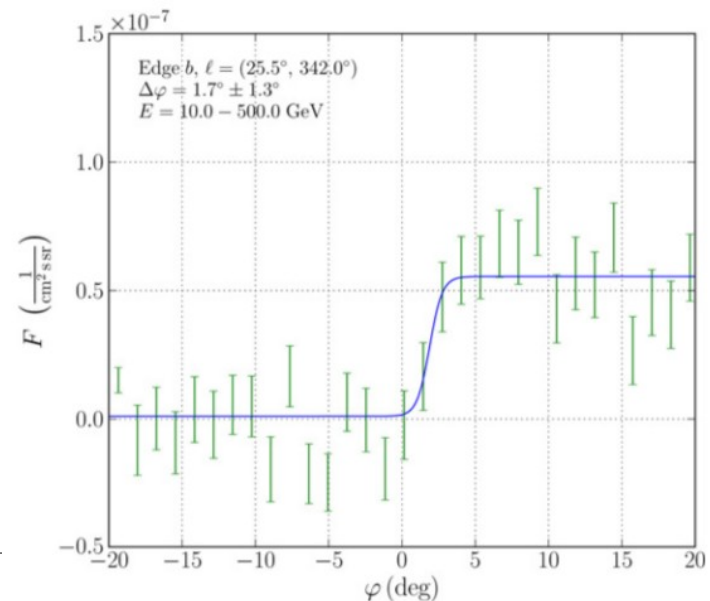
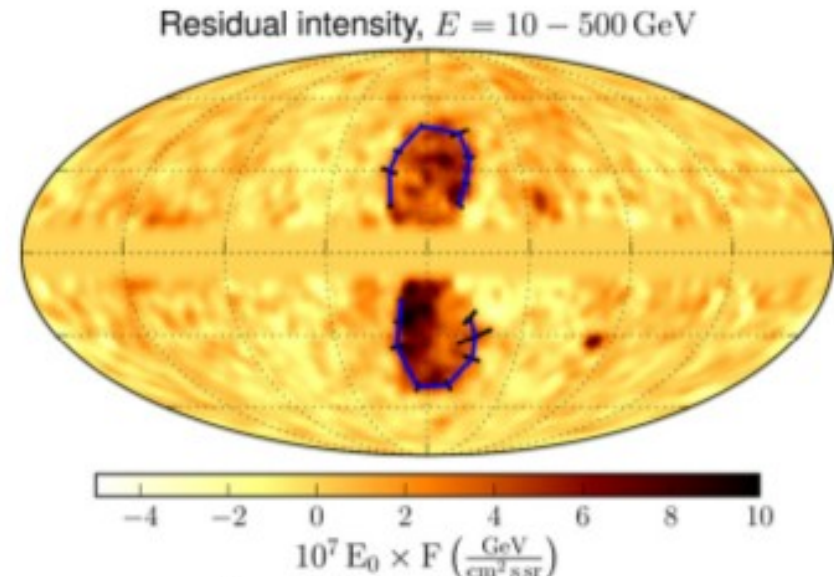
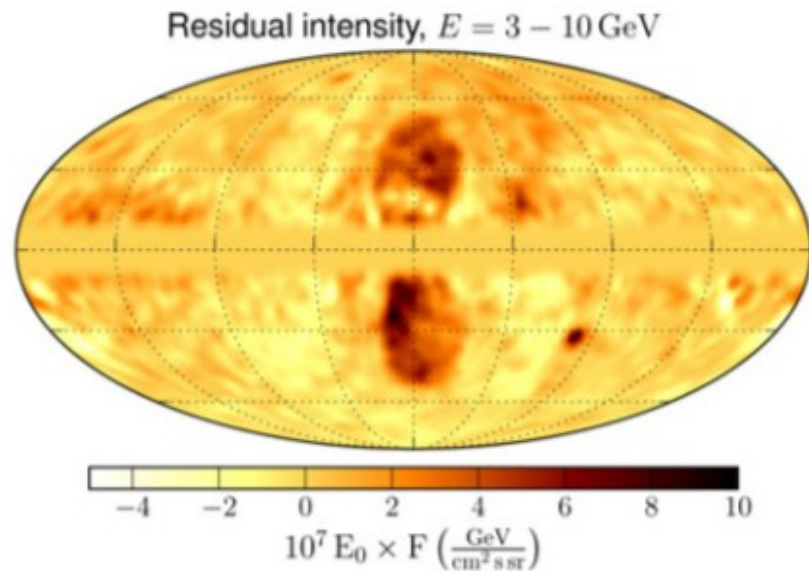
Galactic Centre, which show the expected tracer of the presence of petaelectronvolt protons within the central 10 parsecs of the Galaxy. We propose that the supermassive black hole Sagittarius A* is linked to this PeVatron. Sagittarius A* went through active phases in the past, as demonstrated by X-ray outbursts⁵ and an outflow from the Galactic Centre⁶. Although its current rate of particle acceleration is not sufficient to provide a substantial contribution to Galactic cosmic rays, Sagittarius A* could have plausibly been more active over the last 10^6 – 10^7 years, and therefore should be considered as a viable alternative to supernova remnants as a source of petaelectronvolt Galactic cosmic rays.



Fermi bubbles: Observations

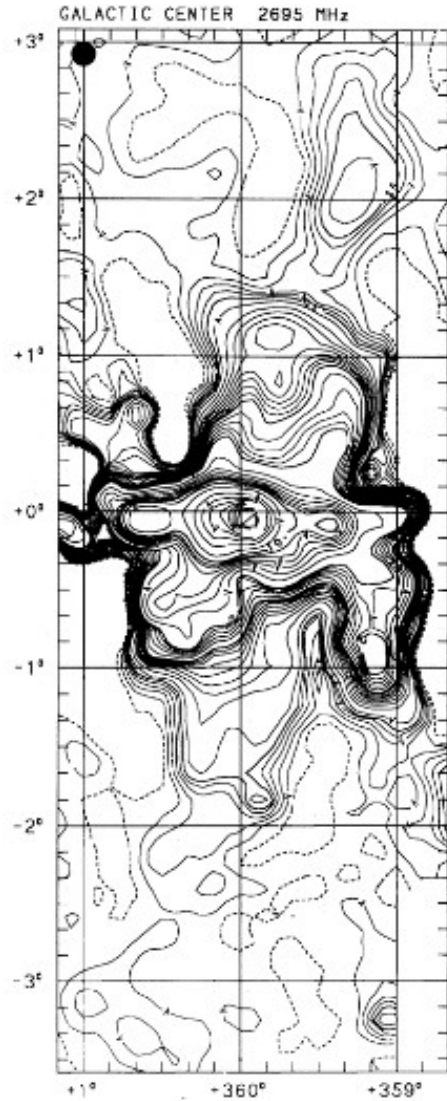
Ackermann et al., ApJ (2014)

- Sharp edges, → Hard spectrum,
- ~ constant surface brightness



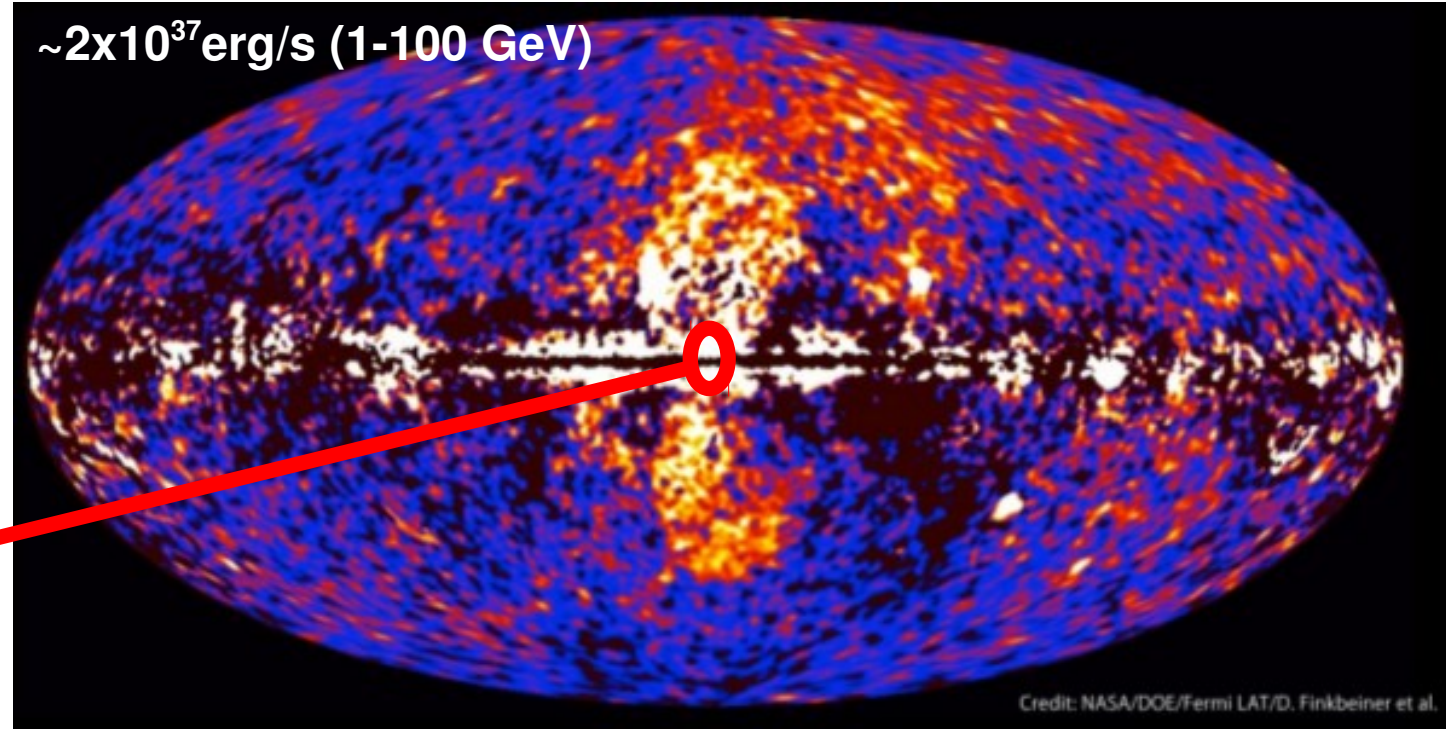
Evidence for an outflow from the GC?

2.7 GHz radio data



Pohl, Reich,
Schlickeiser (1992)

$\sim 2 \times 10^{37}$ erg/s (1-100 GeV)



Credit: NASA/DOE/Fermi LAT/D. Finkbeiner et al.

Su, Slatyer & Finkbeiner (2010)

$U_{\text{outf}} \sim$ a few 100's – 1000 km/s, $P_{\text{outf}} \sim 3 \times 10^{40}$ erg/s

→ SMBH ? *Transient episode, ~ several Myr time-scale*

→ SFR in Central Molecular Zone : 5 – 10 % of MW's massive SF,
SFR density ~ 1000 x avg in MW disk \Rightarrow compatible with P_{outf} , too.

(Crocker et al.) ~ 100 Myr time-scale

→ **Which velocity profile ?**

→ **CRs blown out of GC in this outflow: What happens to them ?**

A leading leptonic model

PRL 107, 091101 (2011)

PHYSICAL REVIEW LETTERS

week ending
26 AUGUST 2011

Fermi Gamma-Ray “Bubbles” from Stochastic Acceleration of Electrons

Philipp Mertsch and Subir Sarkar

Rudolf Peierls Centre for Theoretical Physics, University of Oxford, Oxford OX1 3NP, United Kingdom
(Received 26 April 2011; revised manuscript received 20 May 2011; published 23 August 2011)

Gamma-ray data from Fermi Large Area Telescope reveal a bilobular structure extending up to $\sim 50^\circ$ above and below the Galactic Center. It has been argued that the gamma rays arise from hadronic interactions of high-energy cosmic rays which are advected out by a strong wind, or from inverse-Compton scattering of relativistic electrons accelerated at plasma shocks present in the bubbles. We explore the alternative possibility that the relativistic electrons are undergoing stochastic 2nd-order Fermi acceleration by plasma wave turbulence through the entire volume of the bubbles. The observed gamma-ray spectral shape is then explained naturally by the resulting hard electron spectrum modulated by inverse-Compton energy losses. Rather than a constant volume emissivity as in other models, we predict a nearly constant surface brightness, and reproduce the observed sharp edges of the bubbles.

large-scale, fast-mode turbulence

Cutoff at a few 100 GeV, due to energy-losses

$U \sim 1000$ km/s

Outflow velocity profile ?

Keeney et al., ApJ (2006)

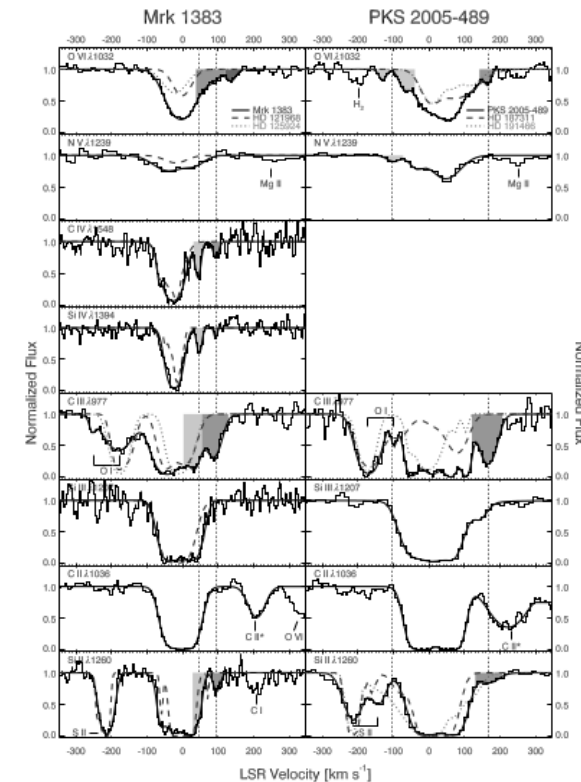
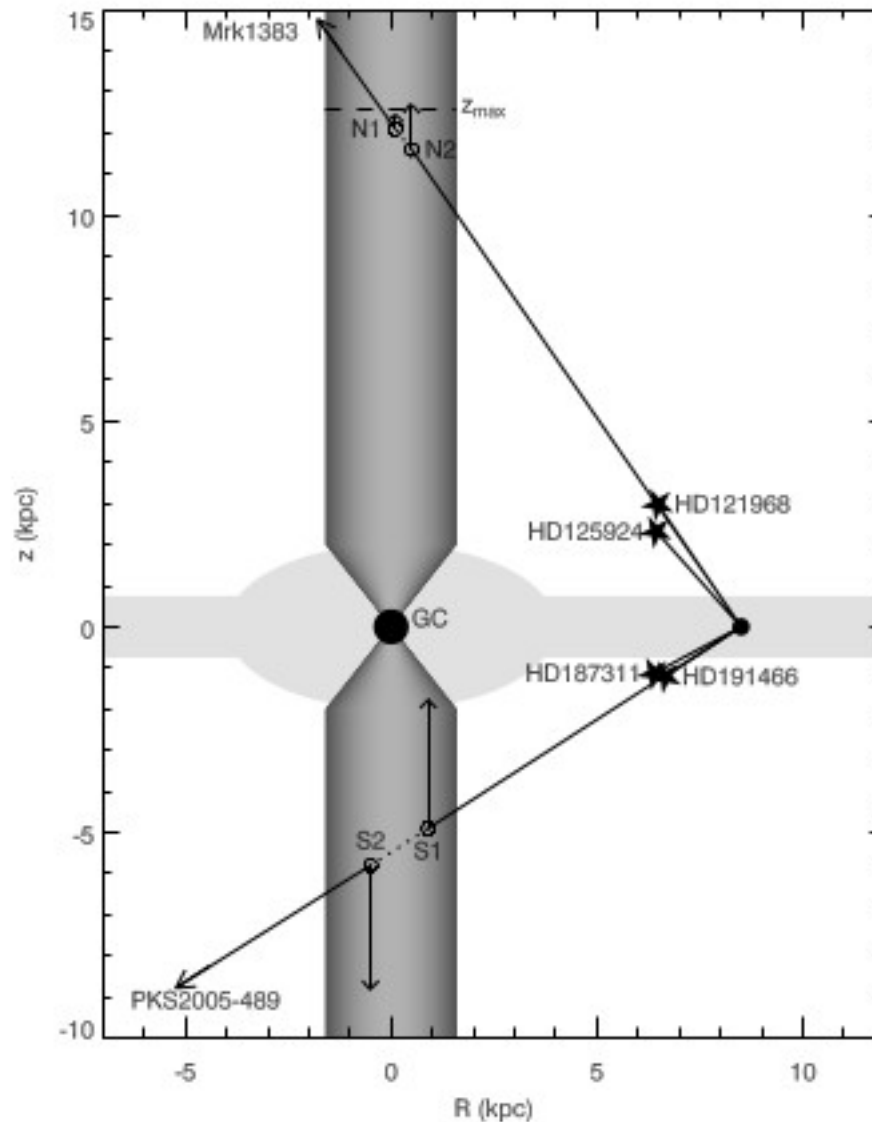
ABSTRACT

We detect high-velocity absorbing gas using *Hubble Space Telescope* and *Far Ultraviolet Spectroscopic Explorer* medium-resolution spectroscopy along two high-latitude active galactic nucleus (AGN) sight lines (Mrk 1383 and PKS 2005–489) above and below the Galactic center (GC). These absorptions are most straightforwardly interpreted as a wind emanating from the GC that does not escape from the Galaxy's gravitational potential. Spectra of four comparison B stars are used to identify and remove foreground velocity components from the absorption-line profiles of O VI, N V, C II, C III, C IV, Si II, Si III, and Si IV. Two high-velocity (HV) absorption components are detected along each AGN sight line, three redshifted and one blueshifted. Assuming that the four HV features trace a large-scale Galactic wind emanating from the GC, the blueshifted absorber is falling toward the GC at a velocity of $250 \pm 20 \text{ km s}^{-1}$, which can be explained by "Galactic fountain" material that originated in a bound Galactic wind. The other three absorbers represent outflowing material; the largest derived outflow velocity is $+250 \pm 20 \text{ km s}^{-1}$, which is only 45% of the velocity necessary for the absorber to escape from its current position in the Galactic gravitational potential. All four HV absorbers are found to reach the same maximum height above the Galactic plane ($|z_{\text{max}}| = 12 \pm 1 \text{ kpc}$), implying that they were all ejected from the GC with the same initial velocity. The derived metallicity limits of $\gtrsim 10\%$ – 20% solar are lower than expected for material recently ejected from the GC unless these absorbers also contain significant amounts of hotter gas in unseen ionization stages.

Constraints on outflow velocity profile

Keeney et al., ApJ (2006)

Absorption lines from partially ionised gas
⇒ Velocity of clumps N1, N2 is ~50 km/s,
And velocity of S1, S2 is ~150 - 250 km/s.



A UNIFIED MODEL OF THE FERMI BUBBLES, MICROWAVE HAZE, AND POLARIZED RADIO LOBES: REVERSE SHOCKS IN THE GALACTIC CENTER'S GIANT OUTFLOWS

ROLAND M. CROCKER^{1,5}, GEOFFREY V. BICKNELL¹, ANDREW M. TAYLOR^{2,6}, AND ETTORE CARRETTI^{3,4}

¹Research School of Astronomy and Astrophysics, Australian National University, Canberra, ACT, Australia

²Dublin Institute of Advanced Studies, Dublin, Ireland

³INAF—Osservatorio di Cagliari, Via della Scienza 5, I-09047 Selargius, Italy

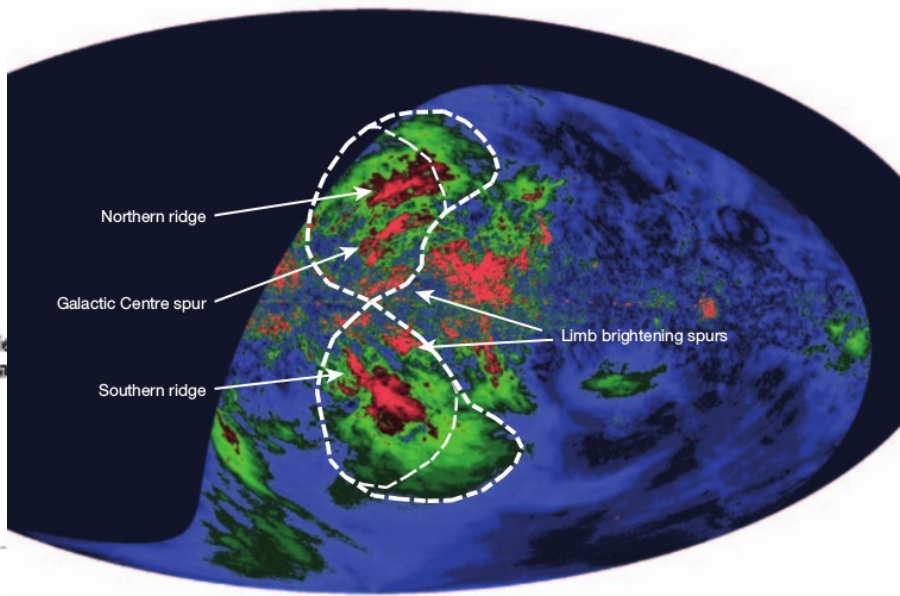
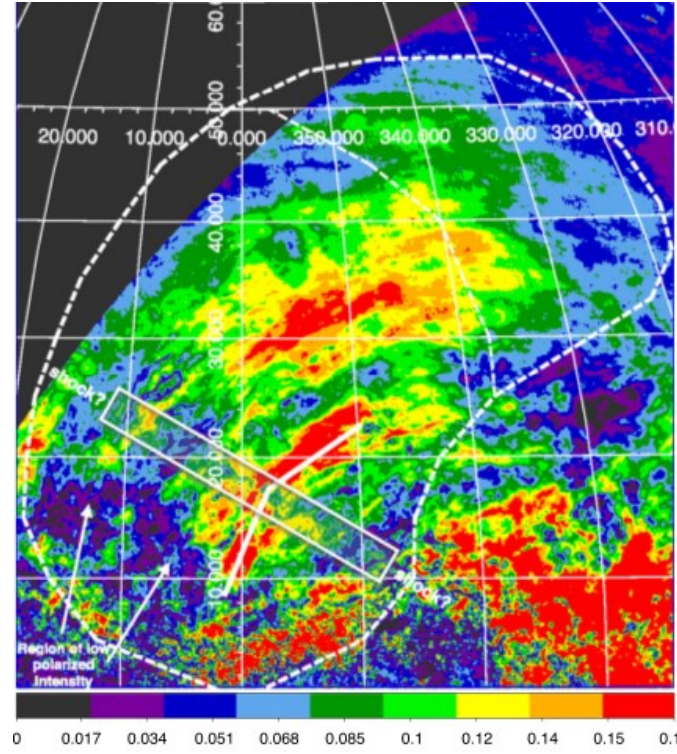
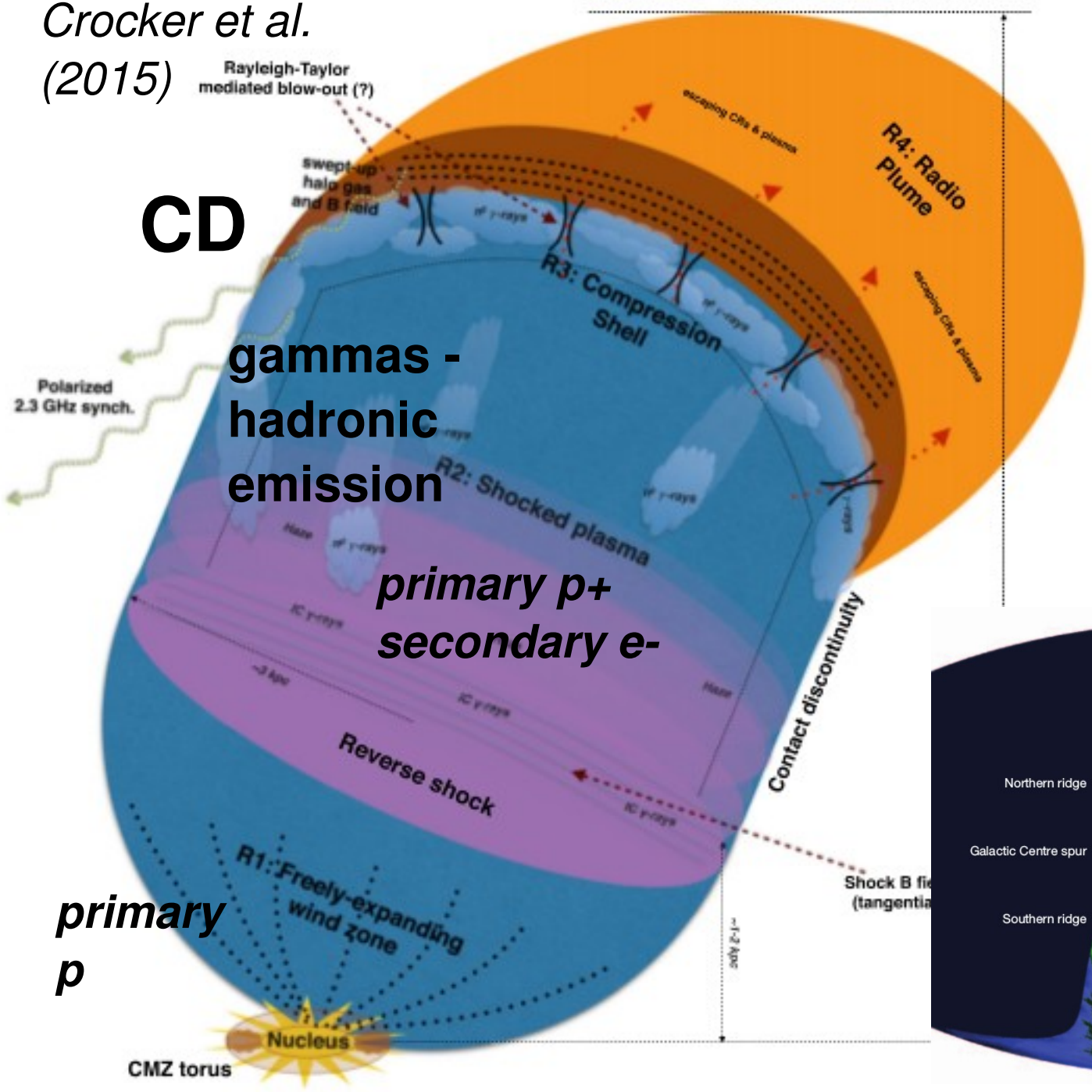
⁴CSIRO Astronomy & Space Science, Marsfield, N.S.W., Australia

Received 2015 April 17; accepted 2015 June 16; published 2015 July 27

ABSTRACT

The Galactic center's giant outflows are manifest in three different, nonthermal phenomena: (1) the hard-spectrum, γ -ray “Fermi bubbles” emanating from the nucleus and extending to $|b| \sim 50^\circ$; (2) the hard-spectrum, total-intensity microwave (~ 20 – 40 GHz) “haze” extending to $|b| \sim 35^\circ$ in the lower reaches of the Fermi bubbles; and (3) the steep-spectrum, polarized, “S-PASS” radio (~ 2 – 20 GHz) lobes that envelop the bubbles and extend to $|b| \sim 60^\circ$. We find that the nuclear outflows inflate a genuine bubble in each Galactic hemisphere that has the classical structure, working outward, of reverse shock, contact discontinuity (CD), and forward shock. Expanding into the finite pressure of the halo and given appreciable cooling and gravitational losses, the CD of each bubble is now expanding only very slowly. We find observational signatures in both hemispheres of giant, reverse shocks at heights of ~ 1 kpc above the nucleus, their presence ultimately explains all three of the nonthermal phenomena mentioned above. Synchrotron emission from shock-reaccelerated cosmic-ray electrons explains the spectrum, morphology, and vertical extent of the microwave haze and the polarized radio lobes. Collisions between shock-reaccelerated hadrons and denser gas in cooling condensations that form inside the CD account for most of the bubbles' γ -ray emissivity. Inverse Compton emission from primary electrons contributes at the 10%–30% level. Our model suggests that the bubbles are signatures of a comparatively weak but sustained nuclear outflow driven by Galactic center star formation over $\gtrsim \text{few} \times 10^8$ yr.

Crocker et al.
(2015)



Carretti 2013 2.3 GHz from S-PASS
CRBTSM 2016, San Vito, Sept 21 (2016)

CR diffusion and advection in a Galactocentric breeze

Taylor & Giacinti, 1607.08862

Diffusion - advection (Monte Carlo) :

$$\frac{\partial \psi_{\text{CR}}}{\partial t} = \nabla \cdot (\mathcal{D} \nabla \psi_{\text{CR}} - \mathbf{V} \psi_{\text{CR}}) + \frac{\partial}{\partial p} \left[\frac{p}{3} (\nabla \cdot \mathbf{V}) \psi_{\text{CR}} \right] - \frac{\psi_{\text{CR}}}{\tau_{pp}} + Q_{\text{CR}}$$

pp loss term

source

$\psi dp = 4\pi p^2 f dp$. CR density per unit of particle momentum p

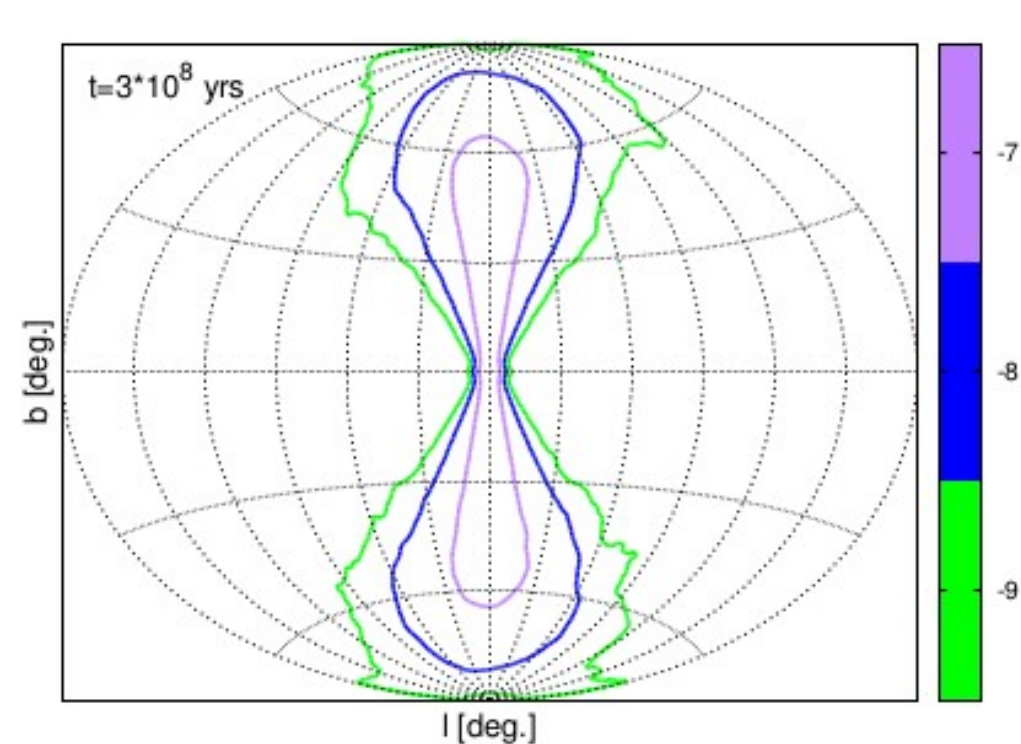
m.f.p. : $\lambda_{10 \text{ GV}} = 3\mathcal{D}_{10 \text{ GV}}/c = 1 \text{ pc}$

Outflow velocity profile : Divergence free with

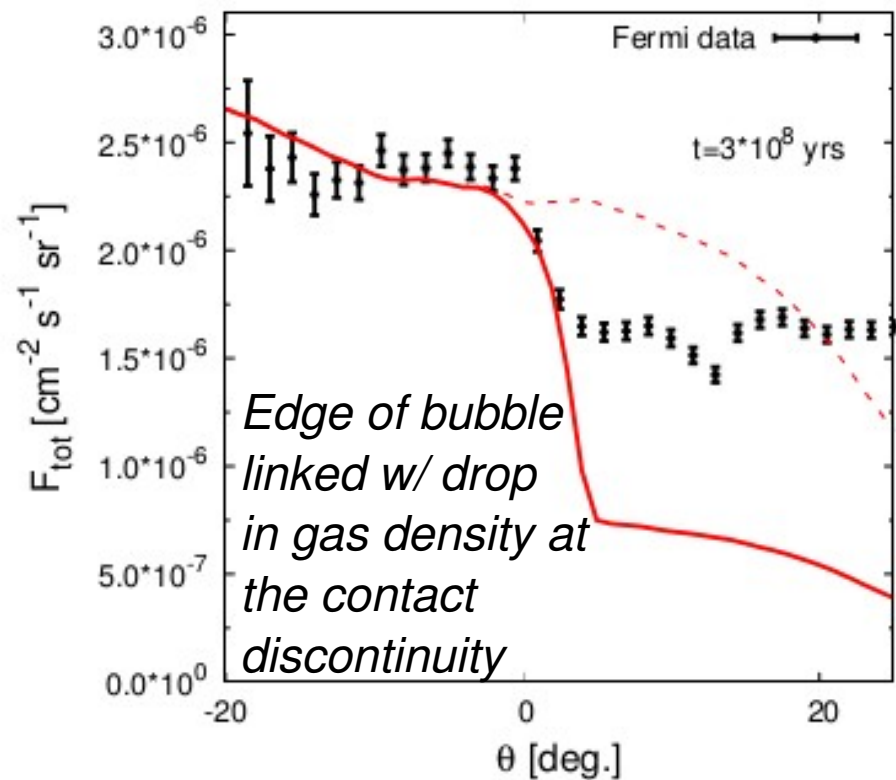
$$\mathbf{V} \cdot \hat{\mathbf{z}} = v_{\text{max}} e^{\frac{1}{2}(1 - \frac{d}{z})} \times \frac{2}{1 + z/d},$$

with $v_{\text{max}} = 300 \text{ km s}^{-1}$ and $d = 1 \text{ kpc}$.

- Timescale of O(100 Myr) to fill a region beyond the bubbles.
- Broadly encapsulates the velocity profile of a “**breeze**” solution for the isothermal outflow problem. The gas density plateaus within the decelerating flow phase. ⇒ motivates ~ **constant density gas in the halo** (~ 10^{-3} cc).



Contour plots for \log_{10} of the γ -ray flux surface brightness ($\text{cm}^{-2} \text{s}^{-1} \text{sr}^{-1}$)

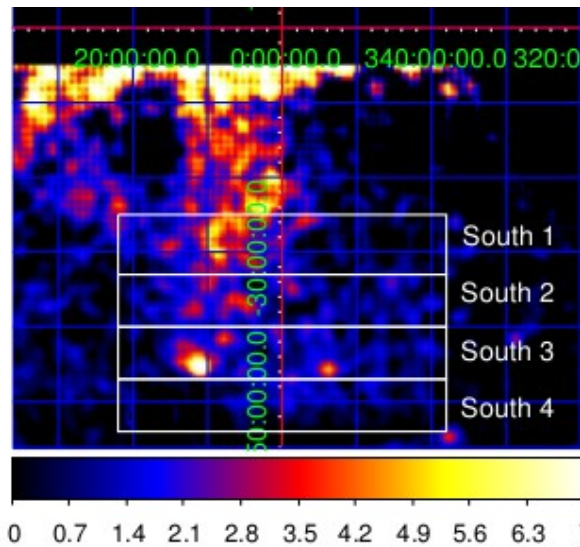


Edge of the 1 – 2 GeV γ -ray bubble from our outflow model with that from the Fermi observation analysis

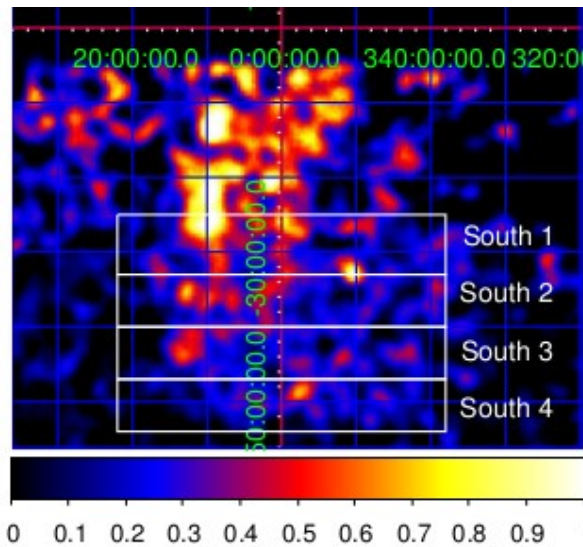
- Morphology + Constant surface brightness well reproduced.
- In general, for cst density gaz, γ -ray data prefers decelerating profiles.
- Sharp edge ↔ Change in gaz density at the CD.
(if not, CR mfp smaller???)
- Explains discrepancy between γ -ray data and 2.3 GHz data. Both p and e- possess extended distributions. Difference in morphology of emission due to differing distributions of target gas and magnetic fields.

Energy spectrum Fermi Bubble South

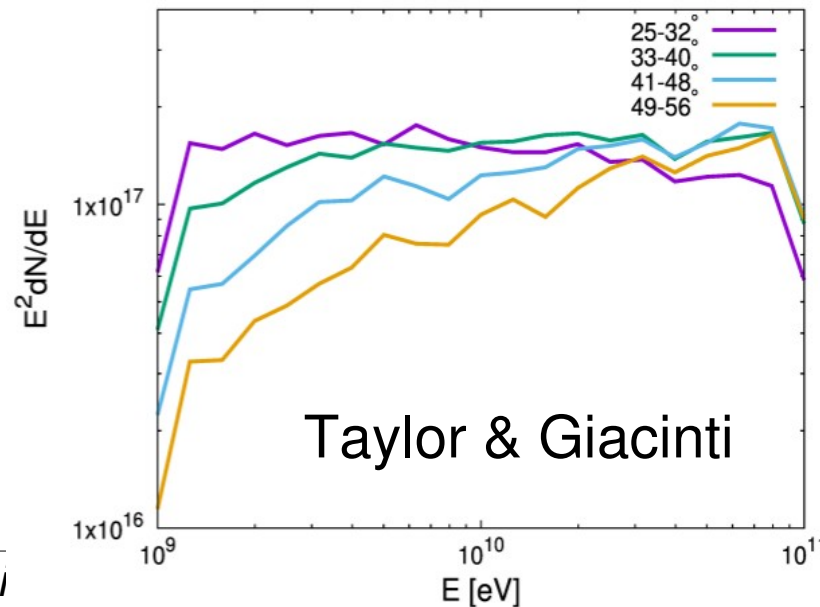
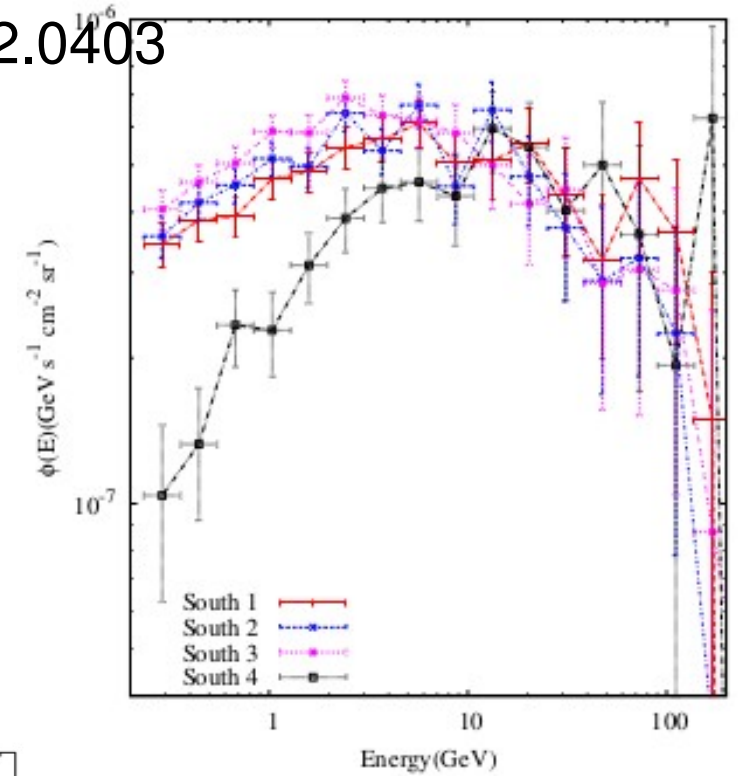
Yang et al., 1402.0403



1 – 2 GeV



10 – 30 GeV



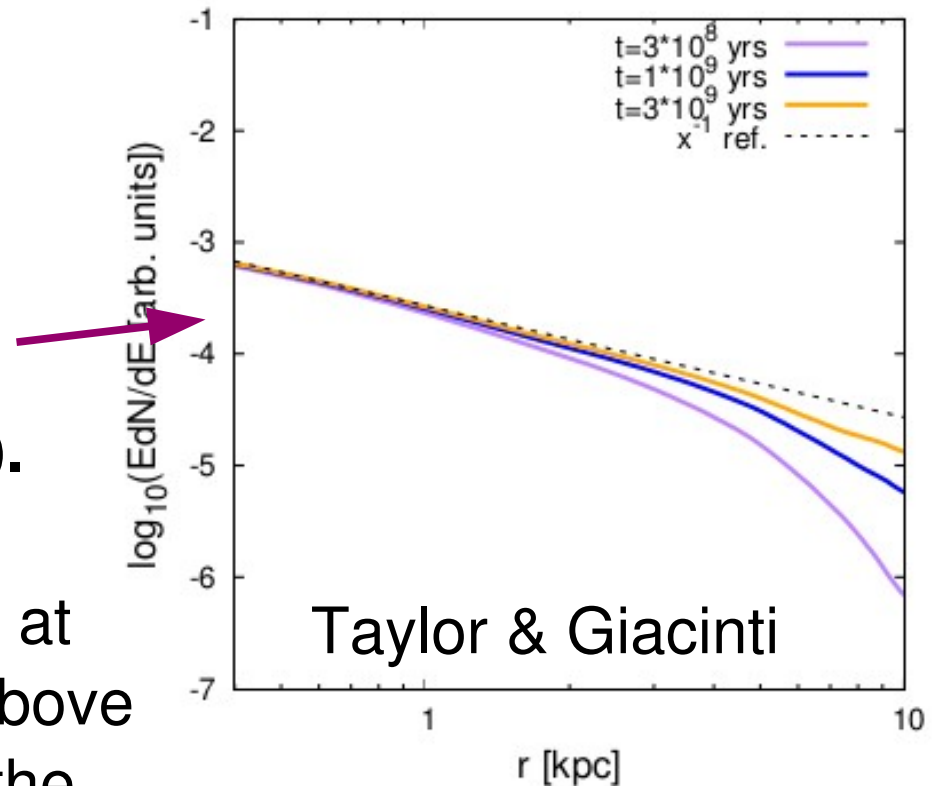
Taylor & Giacinti

PeV CRs at Earth from the GC ?

CR density profile in the disk for **continuous steady injection** of a Galactocentric source and **purely diffusive propagation** (\Rightarrow **Upper limit on contribution**).

HESS paper \Rightarrow 10TeV CR density at **100 pc** from Sgr A* is **~ 6 times** above the sea level. For $1/r$ CR density, the transition distance is **~ 0.6 kpc**.

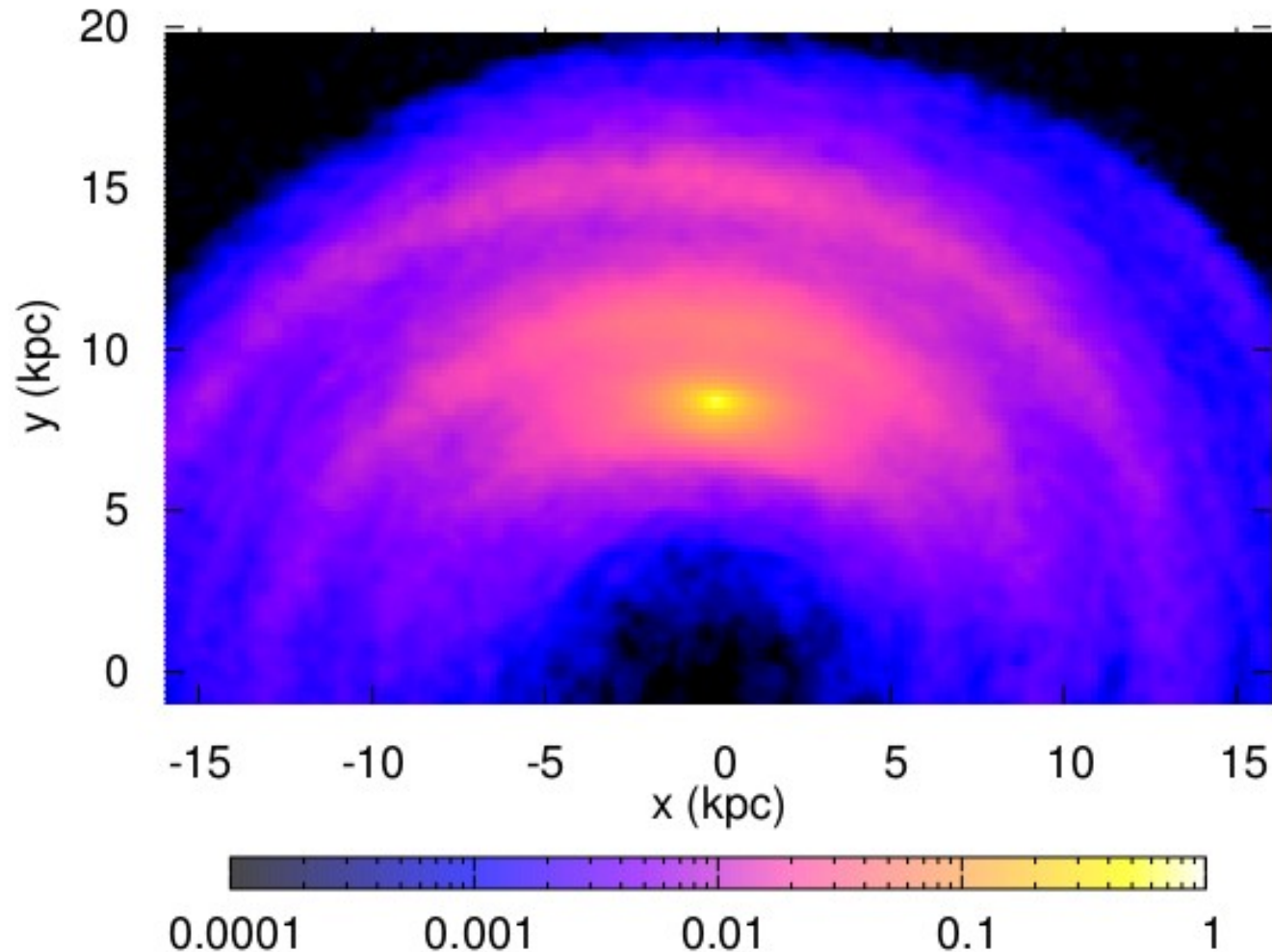
Assuming the CR energy density in the GC region has a spectrum $dN/dE \propto E^{-2.4} \Rightarrow$ Transition at **8 kpc** for **20 PeV $> E_{\text{knee}}$**



Much stronger activity in the past possible, but advection in WIND.

Even without advection : More pessimistic than above estimates

Giacinti et al., JCAP (2012)



Fraction of all particles backtraced from Earth which cross $(200 \text{ pc})^3$ cubes located in the GP region. Earth at $(x, y) = (0, 8.5 \text{ kpc})$, and GC at $(x, y) = (0,0)$. **30 PeV protons**. Pshirkov et al. GMF model.

Conclusions & Perspectives

- Increasing evidence for an outflow produced by the activity at the GC,
- The Fermi bubbles may be the result of CR protons produced from the GC region and advected into the halo. Flat surface brightness reproduced,
- GC not likely to be the source of PeV CRs at Earth. SNe in dense winds better alternative to GC.

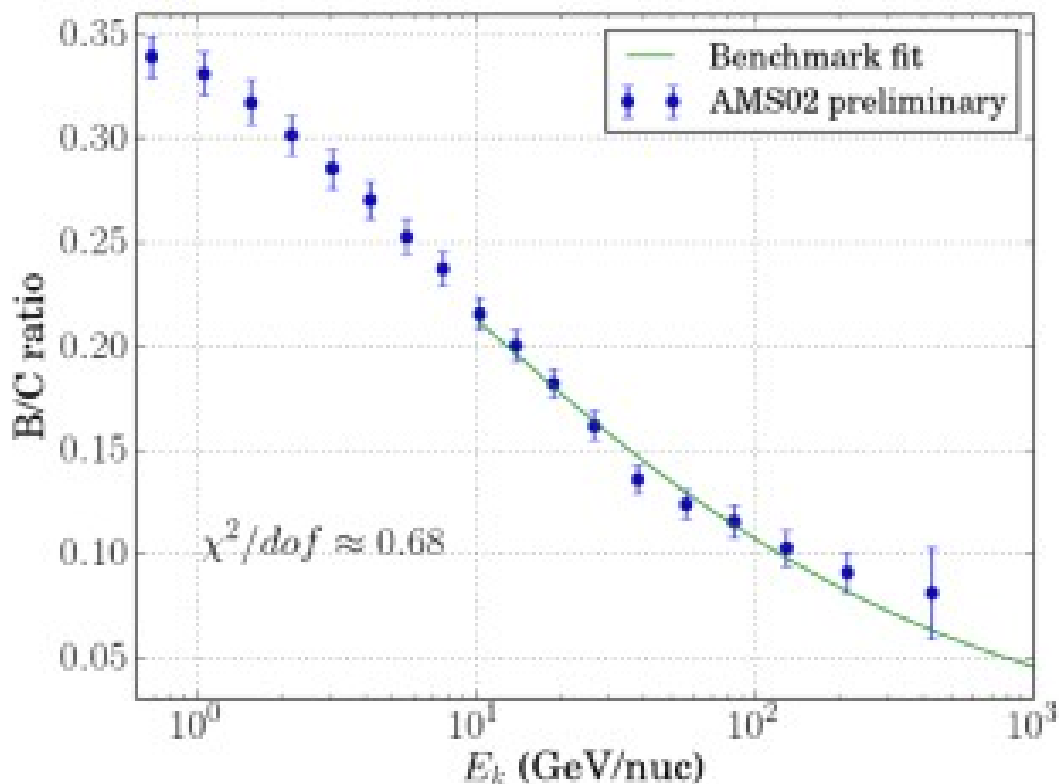
II – GALACTIC WINDS

Giacinti & Taylor, In Prep.

Taylor & Giacinti, arXiv:1607.08862

CR observables / Static halo :

Theoretical uncertainties in extracting cosmic-ray diffusion parameters: the boron-to-carbon ratio

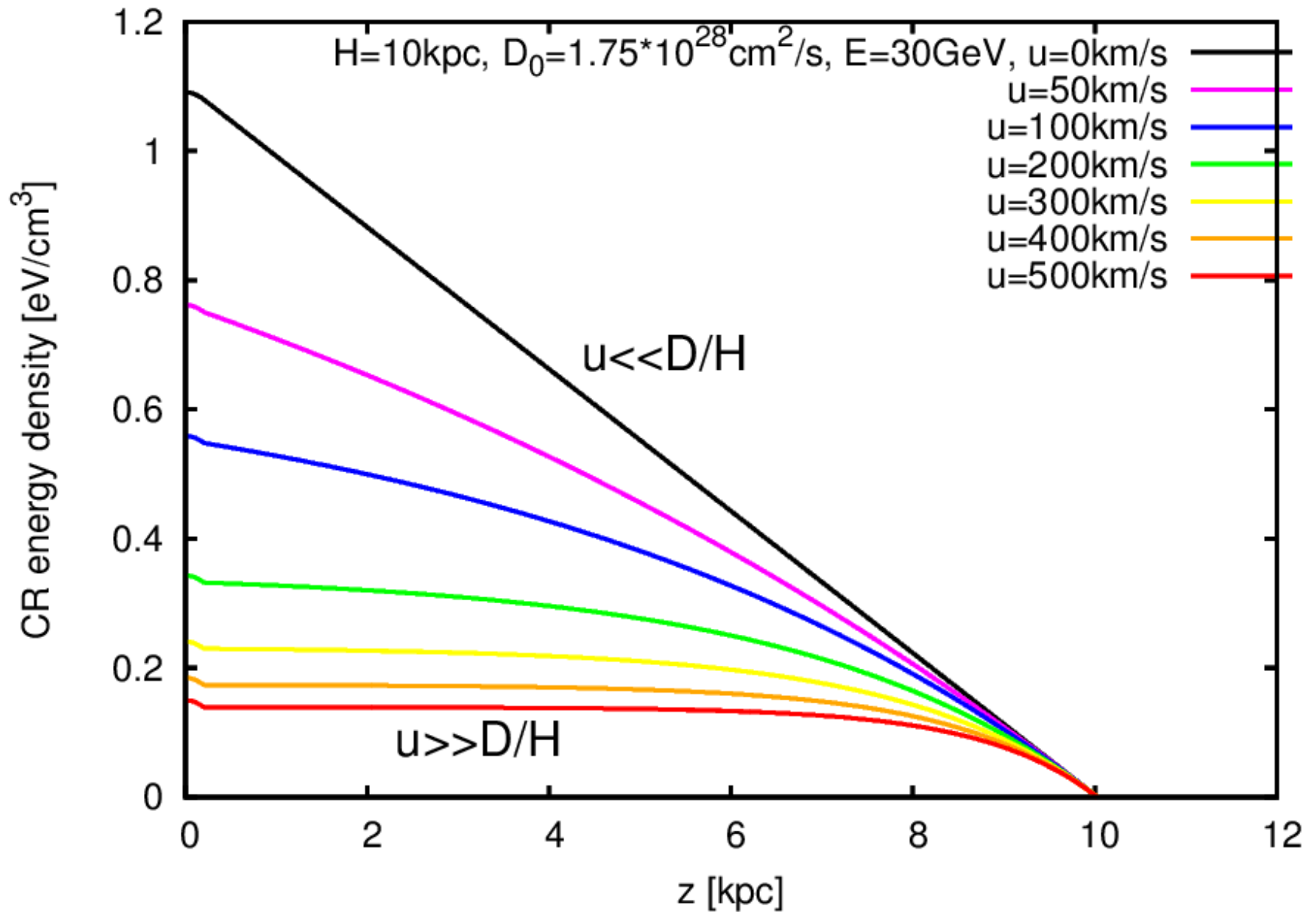


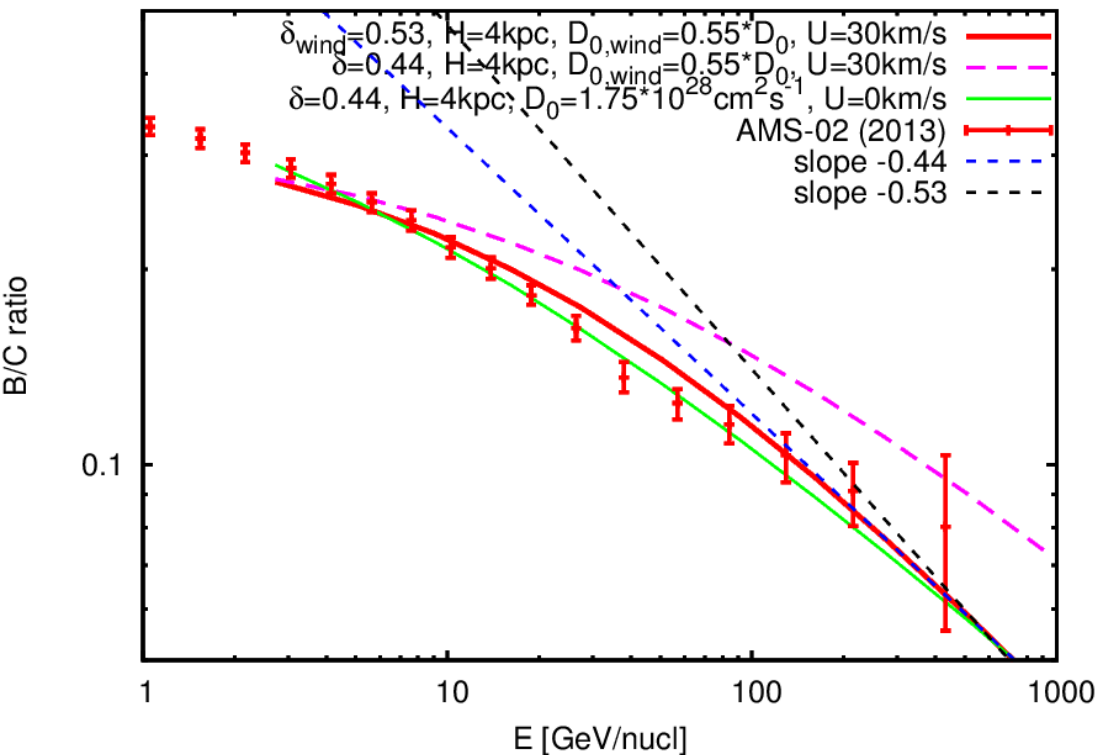
Genolini et al., 1504.03134

Reference parameter values	
α	-2.34
D_0 [kpc ² /Myr]	$(5.8 \pm 0.7) \cdot 10^{-2}$
δ	0.44 ± 0.03
$\chi^2_{B/C}/dof$	$5.4/8 \approx 0.68$
$\gamma = \alpha - \delta$ (fixed)	-2.78

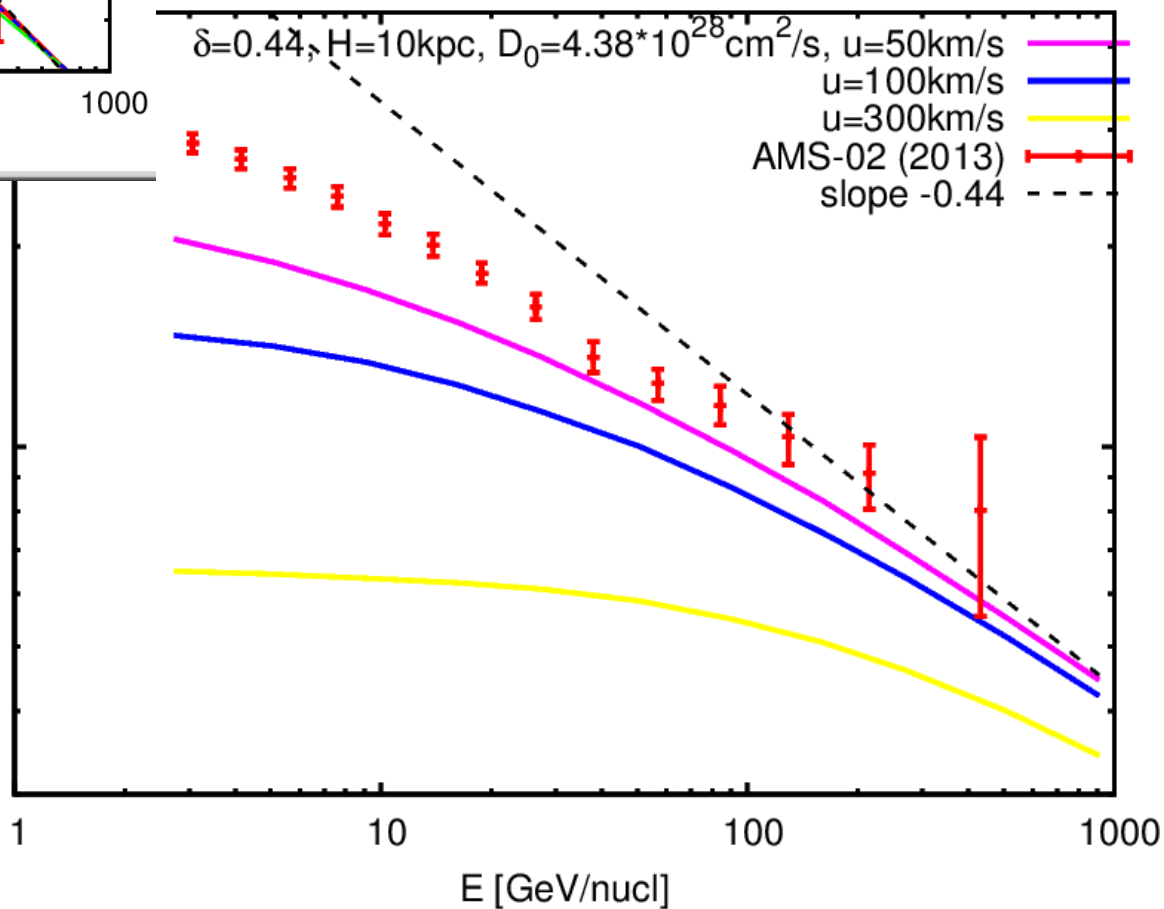
Wind velocity < 30 km/s
(wind velocity constant with z)

Giacinti & Taylor, In prep





Giacinti & Taylor, In prep



$$t_{\text{diff}} \sim z^2/D$$

$$t_{\text{adv}} \sim z/V$$

$$\Rightarrow z_* \sim D/V$$

Advection time prop. to z :

$$z_* \propto D, \text{ here}$$

(low E)

B/C ratio

0.1

E [GeV/nucleon]

Galactic diffusion and wind models of cosmic-ray transport

I. Insight from CR composition studies and γ -ray observations

J.B.G.M. Bloemen^{1,2}, V.A. Dogiel³, V.L. Dorman³, and V.S. Ptuskin⁴

$$-\frac{\partial}{\partial z} \left(D(E) \frac{\partial}{\partial z} N - V N \right) - \frac{\partial}{\partial E} \left(\frac{1}{3} \frac{dV}{dz} E N \right) = Q(E, z)$$

with

$$D(E) = D_0 E^\alpha,$$

$$V(z) = 3 V_0 z,$$

$$Q(E, z) = 2 z_s K E^{-\gamma_0} \delta(z)$$

$$t_{\text{diff}} \sim z^2/D$$

$$t_{\text{adv}} \sim z/V$$

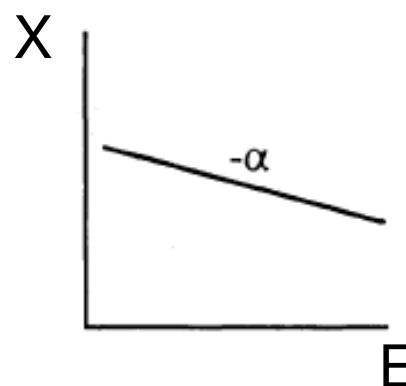
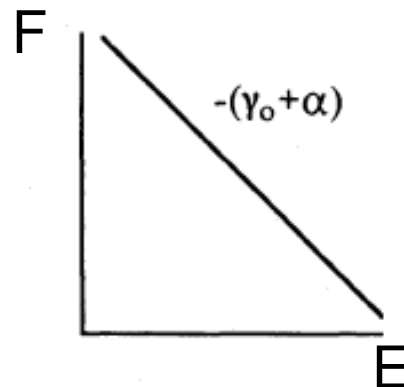
$$\Rightarrow z_* \sim D/V$$

Advection time is independent of z :

$$z_* \propto D^{1/2}, \text{ here}$$

DIFFUSION MODEL ($z=0$)

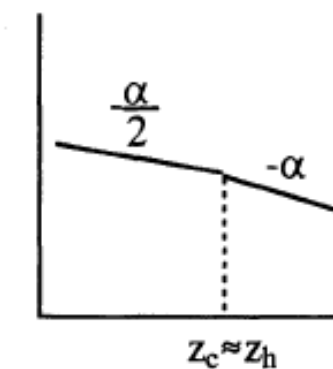
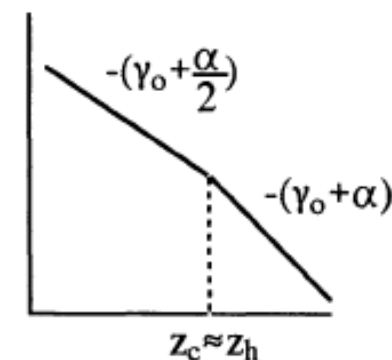
$$D(E) \propto E^\alpha \text{ and } z_h$$



CONVECTION-DIFFUSION MODEL ($z=0$)

$$D(E) \propto E^\alpha, z_h \text{ and } V_0$$

$$z_c(E) = \sqrt{\frac{2D_0 E^\alpha}{(3 + \alpha/2)V_0}}$$

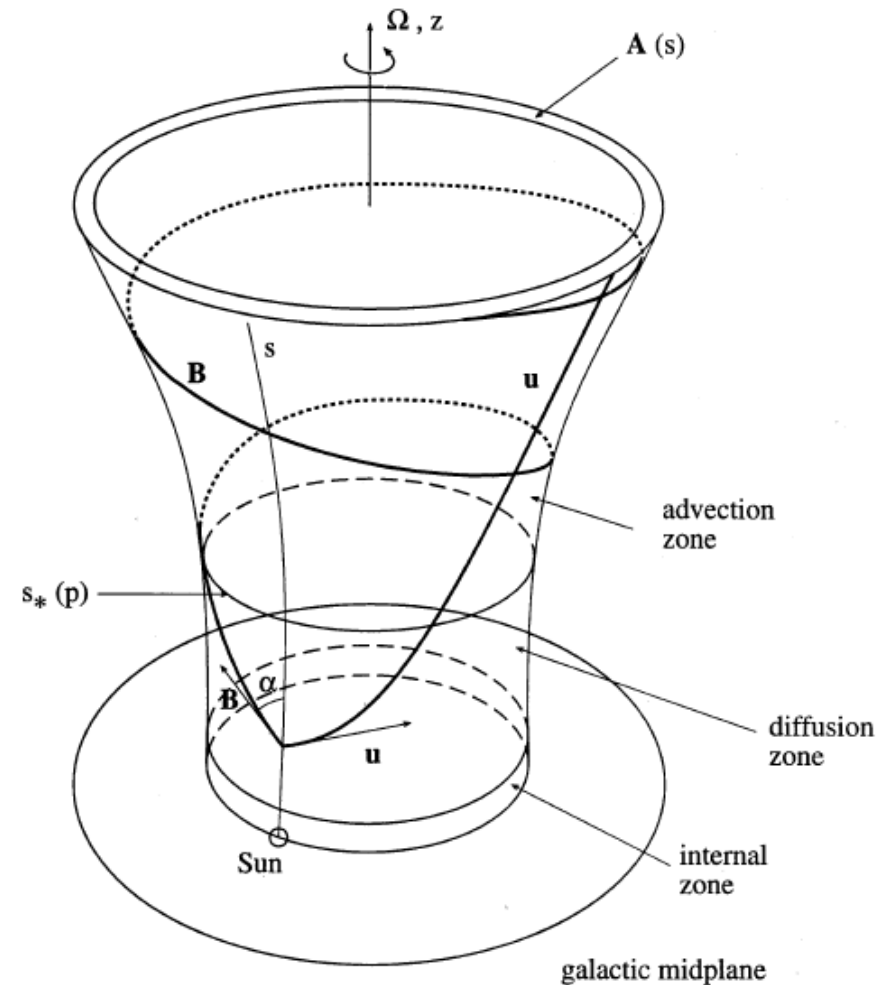


See also *P. Blasi's talk*

Transport of relativistic nucleons in a galactic wind driven by cosmic rays

V.S. Ptuskin¹, H.J. Völk², V.N. Zirakashvili¹, and D. Breitschwerdt^{2,3}

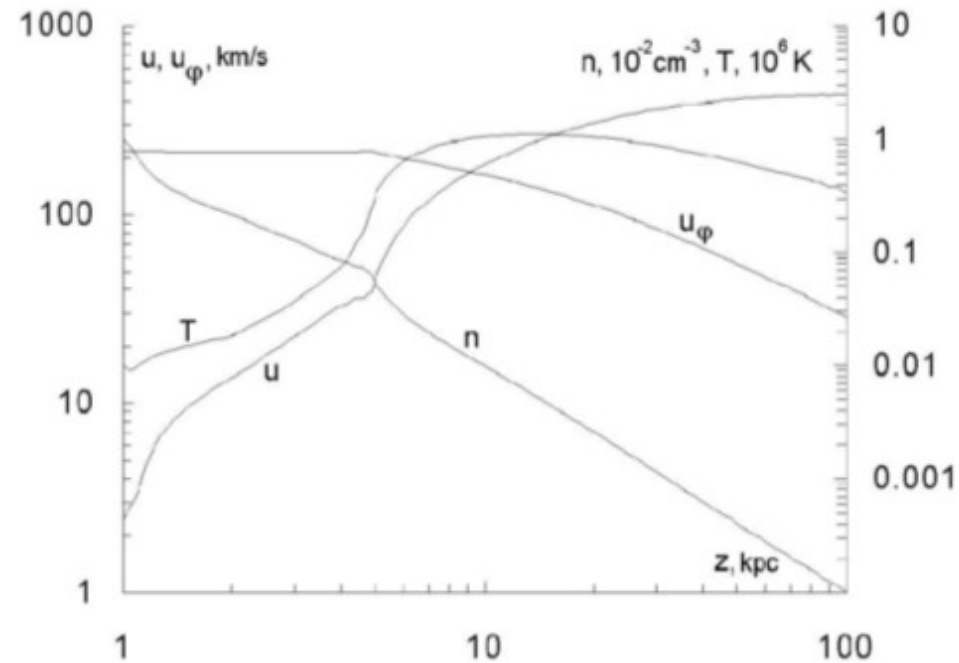
Abstract. For the first time an attempt is made at a self-consistent analytical description of the halo structure and the propagation of energetic particles in late type galaxies like our own. Galactic CR are produced together with hot gas by sources deep in the disk. This leads to a galactic wind and magnetohydrodynamic fluctuations (excited by the cosmic-ray streaming instability) which in turn together determine the transport of these energetic particles into intergalactic space. Wave excitation is balanced locally by nonlinear Landau damping. The cosmic-ray transport equations for the dominant nucleons are solved in an approximate form analytically. Although fully nonlinear, the resulting picture is simple and corresponds to an overall spatial structure that extends to distances considerably greater than the radius of the galactic disk. The inferred source spectrum for cosmic-ray nucleons is a rather hard power law in energy, of index ~ 2.1 . The observed abundances of secondary nuclei are also consistent with this model. The observed disk-halo transition at distances ~ 1 kpc is an important part of the detailed picture in which ion neutral friction damps short-scale magnetic fluctuations below that level.



$$(u + v_a)s_* \sim D_{\parallel} \cos^2 \alpha.$$

At distances smaller than the Galactic radius R_g CRs are advected with Alfvén velocity that is approximately proportional to the height s . The height of diffusion-advection boundary is then $s_*(p) \propto p^{(\gamma-3)/2}$. The spectrum in the disk is $N_{obs}(p) \propto Q(p)/v_a(s_*) \propto p^{-\frac{3}{2}(\gamma-1)}$.

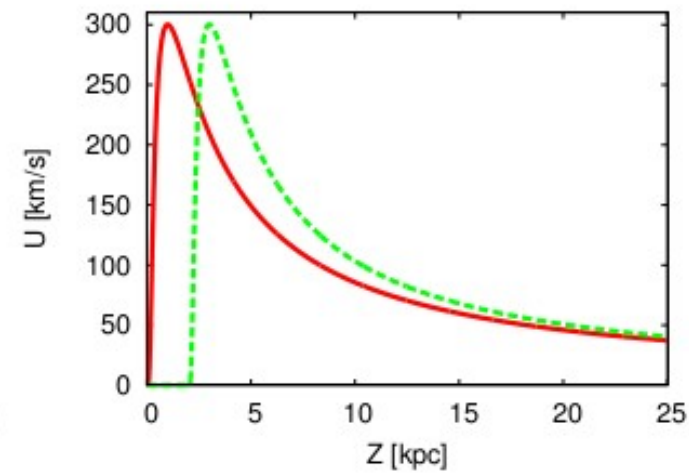
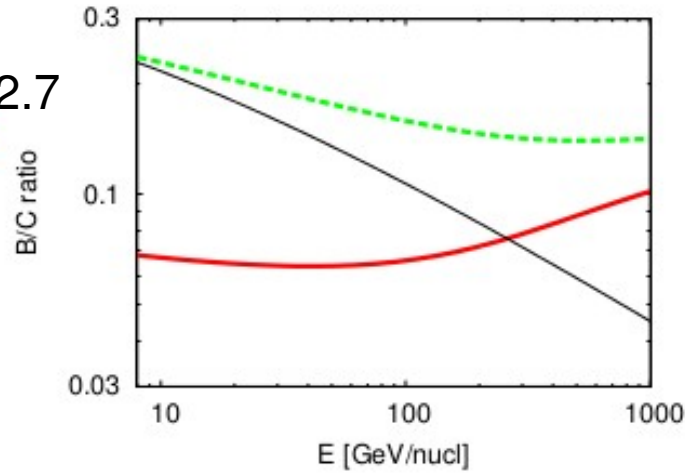
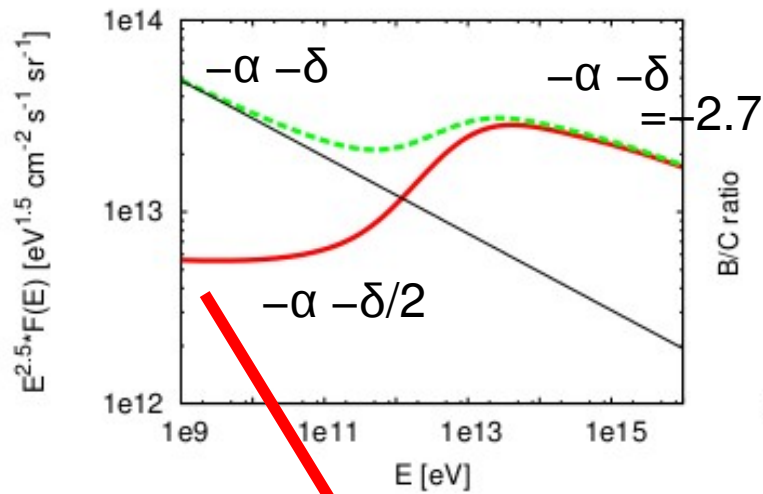
At large distances CR particles are advected by the wind with almost constant speed, the magnetic field is almost azimuthal and $\cos \alpha \propto s^{-1}$. This gives the distance to the diffusion-advection boundary $s_*(p) \propto p^{(\gamma-3)/3}$. The observable spectrum $N_{obs} \propto Q(p)/us_*^2 \propto p^{-\frac{5}{3}\gamma+2}$.



$$N_{obs}(p) \propto \begin{cases} p^{-\frac{3}{2}(\gamma-1)}, & p < p_g \\ p^{-\frac{5}{3}\gamma+2}, & p > p_g \end{cases}$$

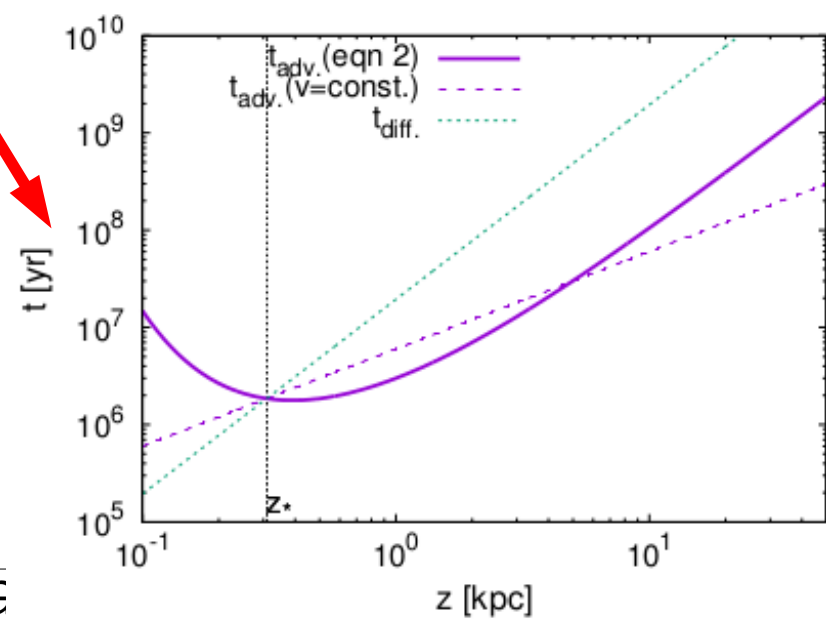
Taylor & Giacinti

$$D = D_{10 \text{ GV}} (E / (Z \times 10 \text{ GV}))^\delta, \quad \delta \rightarrow 1/3$$



$D_{10 \text{ GV}} = 3 \times 10^{28} \text{ cm}^2 \text{ s}^{-1}$, $\delta = 1/3$, $H = 25 \text{ kpc}$, $n(z) = 0.85 \text{ cm}^{-3}$ for $|z| \leq h$ and 10^{-3} cm^{-3} otherwise, CR spectrum at sources $\propto E^{-2.37}$, and total power injected in CRs at $|z| \leq h$ set to $\approx 3.3 \times 10^{39} \text{ erg pc}^{-2} \text{ yr}^{-1}$.

t_{diff} and z_* are shown here for **10 GV CR**.

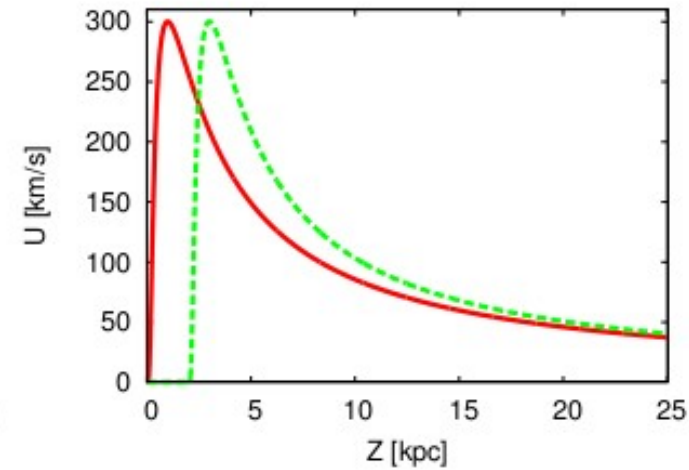
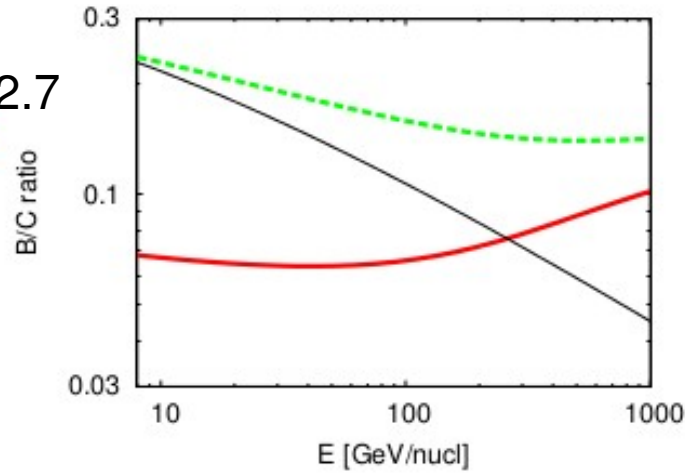
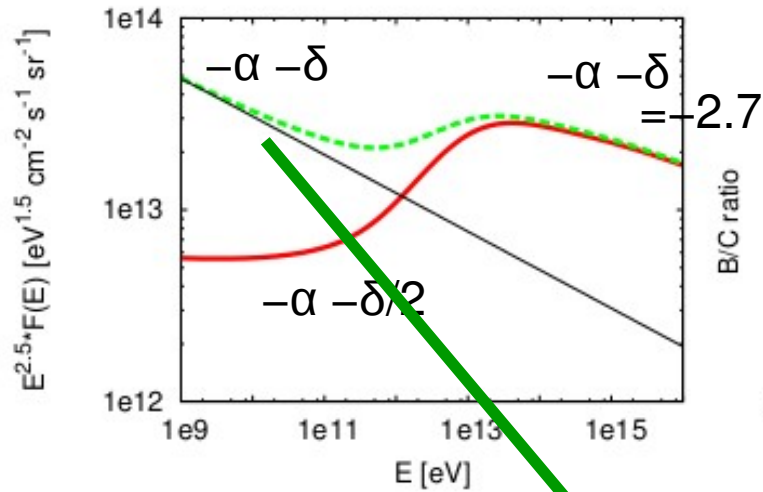


$$z_* \propto D^\beta$$

- low E : $\beta \sim 0.5$
"Bloemen-like" wind
- higher E : $\beta \gg 1$
→ sees the full halo
"leaky box"

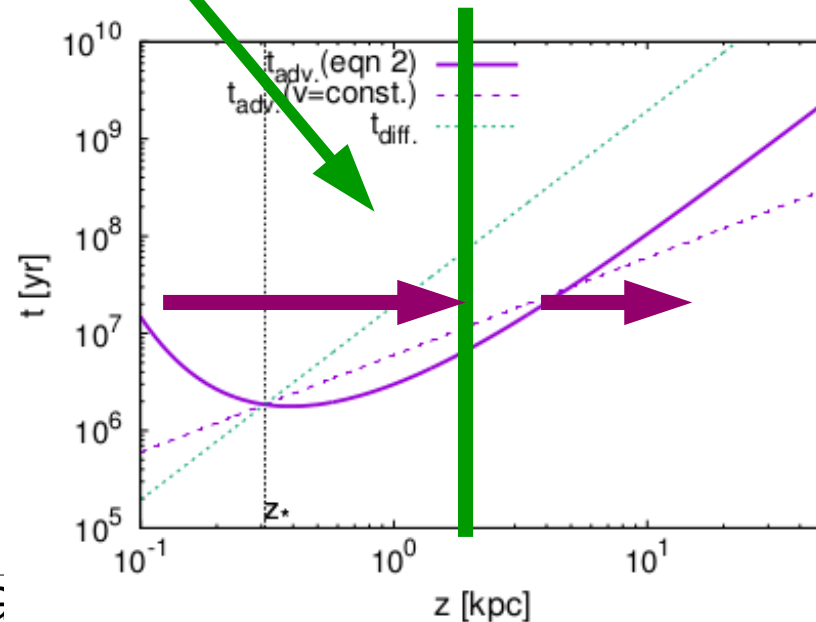
Taylor & Giacinti

$$D = D_{10 \text{ GV}} (E / (Z \times 10 \text{ GV}))^\delta, \quad \delta \rightarrow 1/3$$



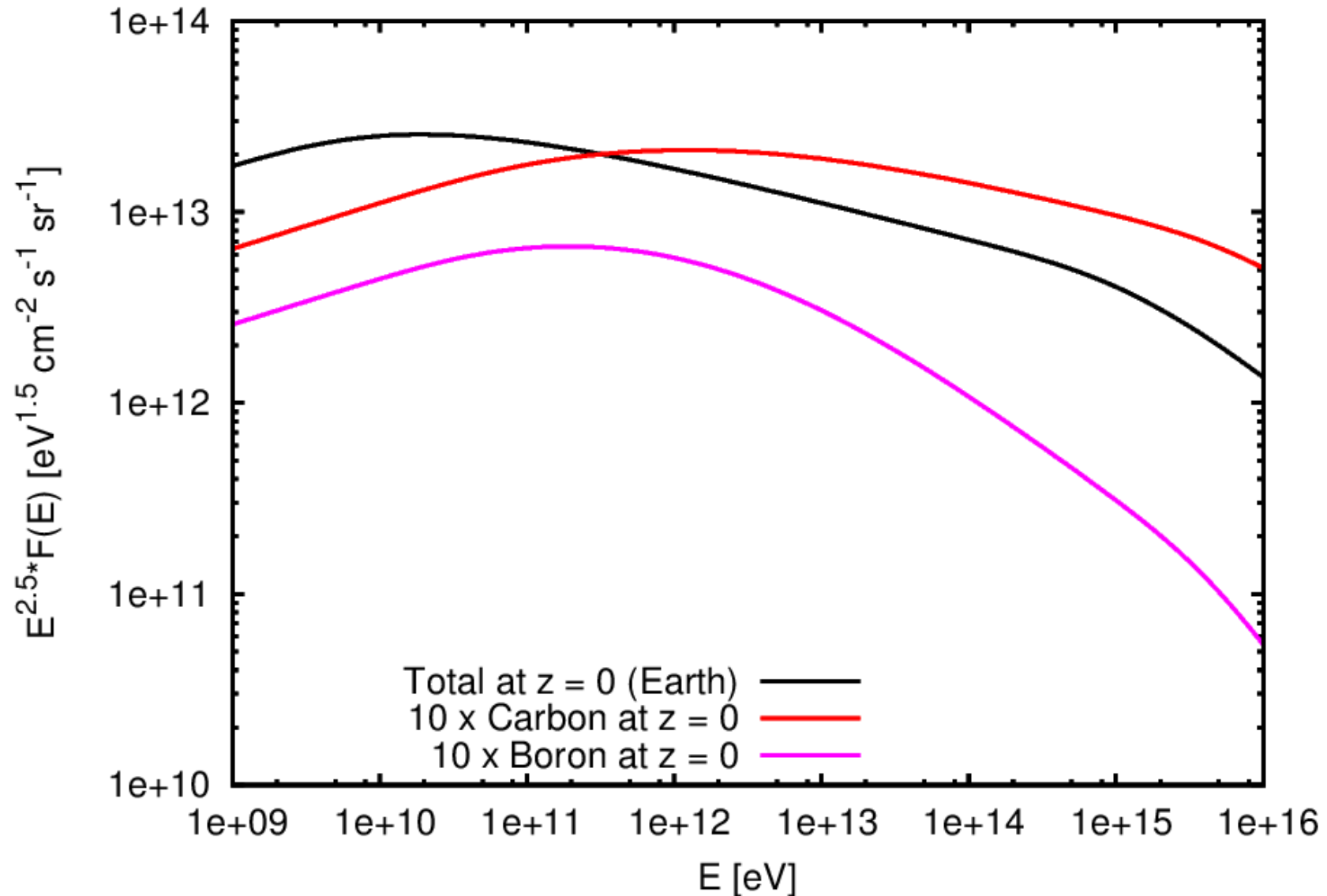
$D_{10 \text{ GV}} = 3 \times 10^{28} \text{ cm}^2 \text{ s}^{-1}$, $\delta = 1/3$, $H = 25 \text{ kpc}$, $n(z) = 0.85 \text{ cm}^{-3}$ for $|z| \leq h$ and 10^{-3} cm^{-3} otherwise, CR spectrum at sources $\propto E^{-2.37}$, and total power injected in CRs at $|z| \leq h$ set to $\approx 3.3 \times 10^{39} \text{ erg pc}^{-2} \text{ yr}^{-1}$.

t_{diff} and z_* are shown here for **10 GV CR**.

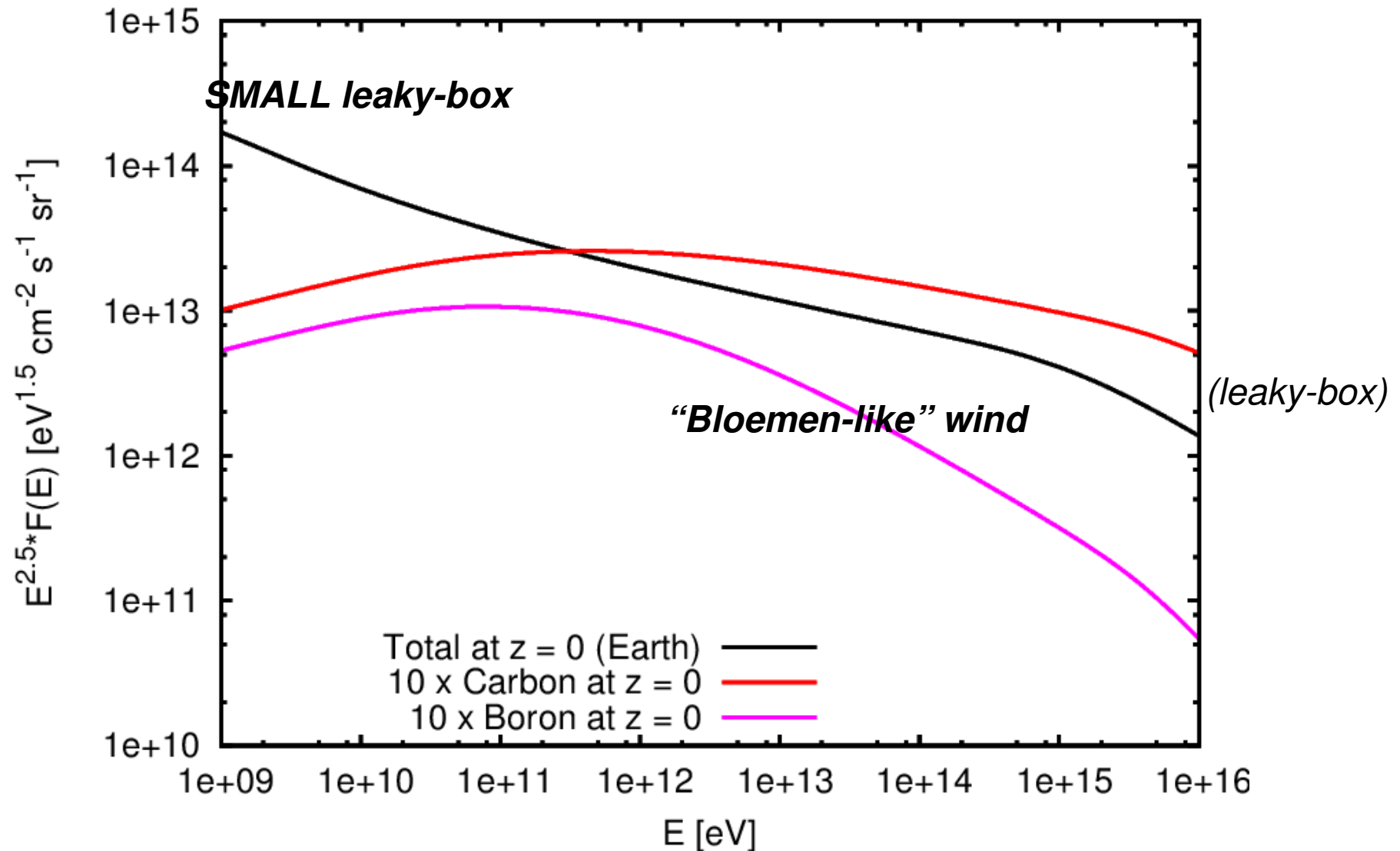


- low E : sees a SMALL leaky-box
- higher E :
 - sees the full halo "leaky box"

And with a proper WIND:



And with a proper WIND:

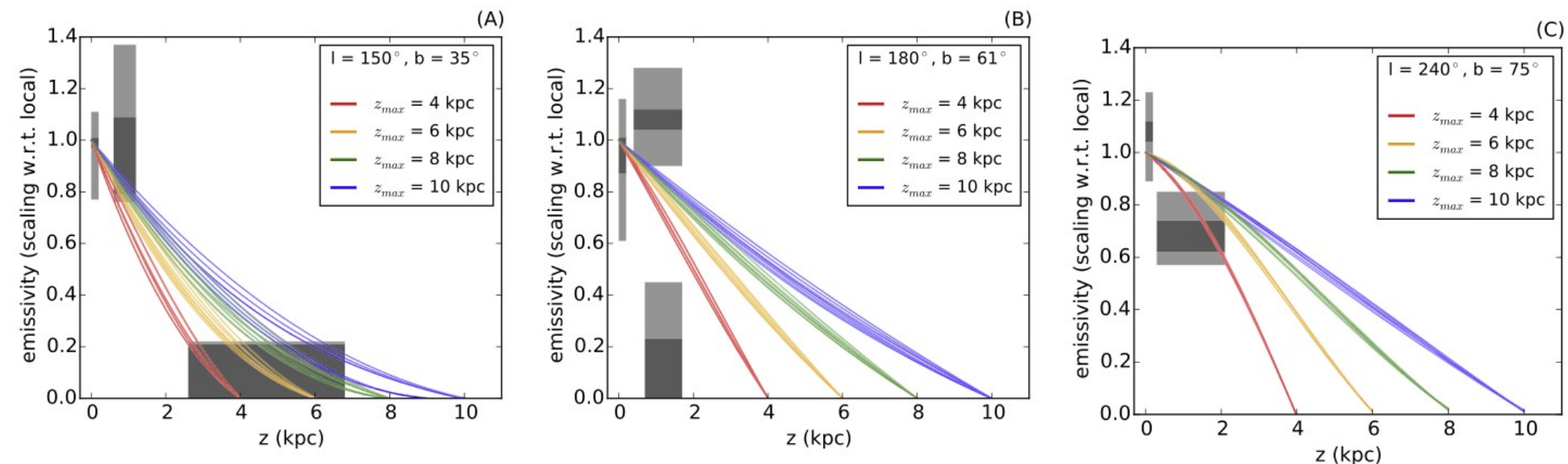


Hardening at low E, even with $D(z)=cst$ → AMS data ?

FERMI-LAT OBSERVATIONS OF HIGH- AND INTERMEDIATE-VELOCITY CLOUDS: TRACING COSMIC RAYS IN THE HALO OF THE MILKY WAY

L. TIBALDO¹, S. W. DIGEL¹, J. M. CASANDJIAN², A. FRANCKOWIAK¹, I. A. GRENIER², G. JÓHANNESSEN³, D. J. MARSHALL²,
I. V. MOSKALENKO¹, M. NEGRO^{1,4}, E. ORLANDO¹, T. A. PORTER¹, O. REIMER^{1,5}, AND A. W. STRONG⁶

Fermi Large Area Telescope in the energy range between 300 MeV and 10 GeV to search for γ -ray emission produced by CR interactions in several high- and intermediate-velocity clouds (IVCs) located at up to ~ 7 kpc above the Galactic plane. We achieve the first detection of IVCs in γ rays and set upper limits on the emission from the remaining targets, thereby tracing the distribution of CR nuclei in the halo for the first time. We find that the γ -ray emissivity per H atom decreases with increasing distance from the plane at 97.5% confidence level. This corroborates the notion that CRs at the relevant energies originate in the Galactic disk. The emissivity of the upper intermediate-velocity Arch hints at a 50% decline of CR densities within 2 kpc from the plane. We compare our results to predictions of CR propagation models.



Conclusions & Perspectives

- Inclusion of a Galactic wind has dramatic consequences on the deduced Galactic CR propagation parameters,
- \Rightarrow Better understanding of CR propagation in the HALO crucial.

Solution : e.g. Tibaldo et al., other avenues ?

- Softenings, but also **hardenings** possible, even in the limiting case of $D(z)=\text{cst}$.

*May relate to the **200 GV** hardening observed in the CR spectrum by AMS.*

COSMIC-RAY ANISOTROPY AS A PROBE OF INTERSTELLAR TURBULENCE

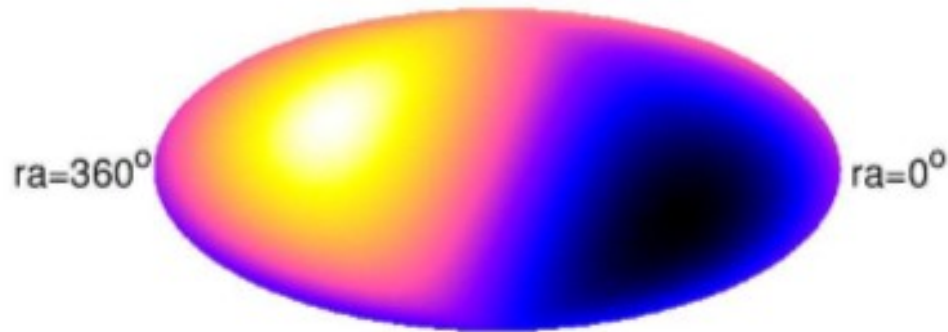
Gwenael Giacinti (MPIK Heidelberg)

&

John G. Kirk (MPIK Heidelberg)

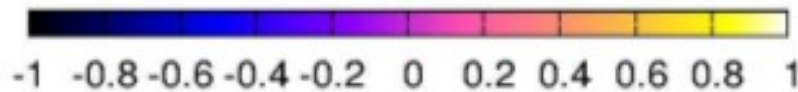
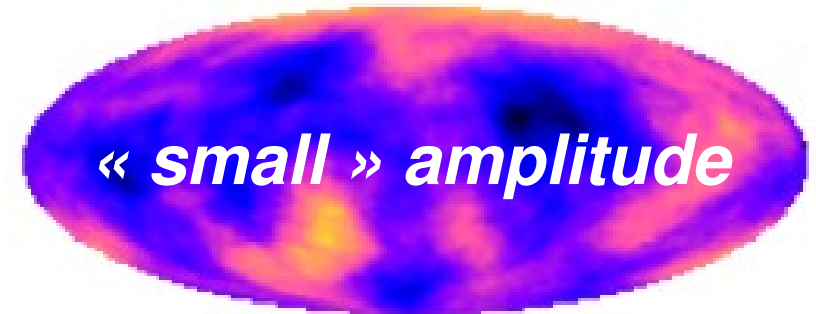
Cosmic-Ray Anisotropy

large-scale



small-scales

+



See Ahlers (2016)

- In the direction of field lines
- Amplitude
- **Shape** (... Dipole ?)



See e.g. Giacinti & Sigl (2012)

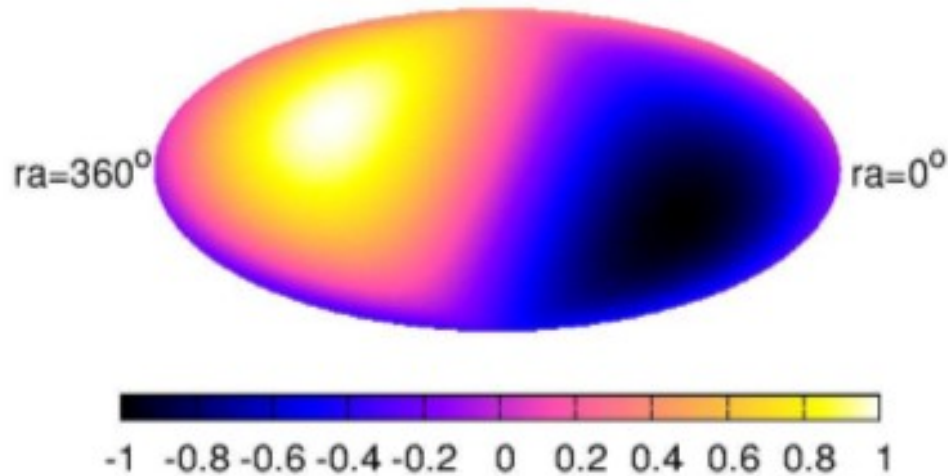
Drury (2013)

Ahlers (2014)

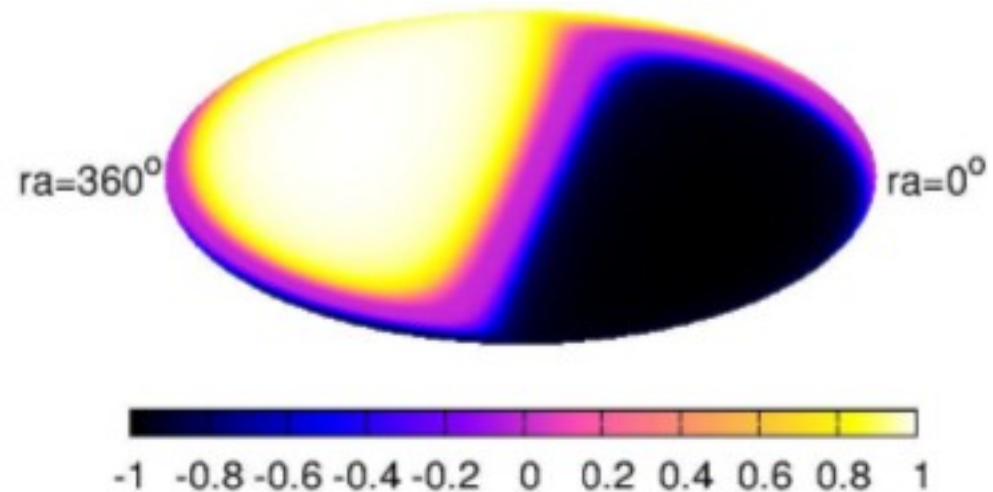
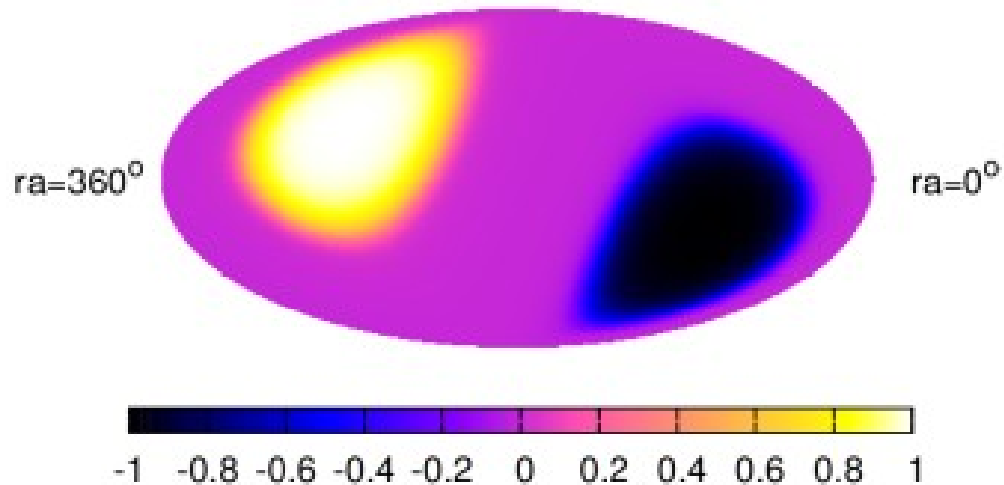
Malkov et al. (2010)

Cosmic-Ray Anisotropy

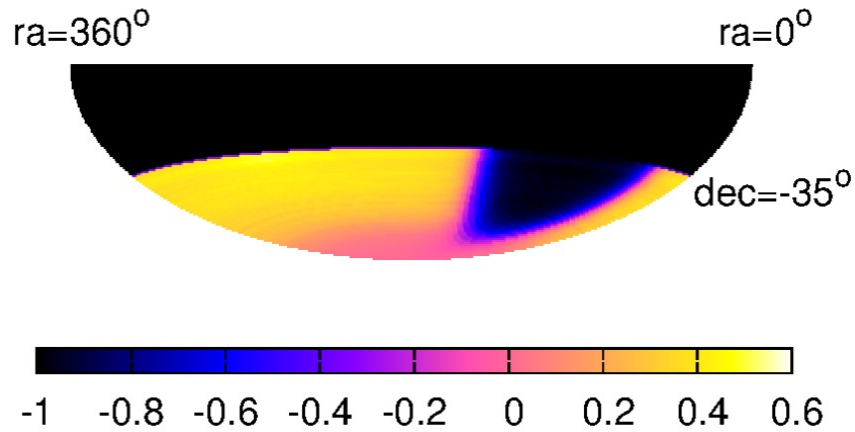
Dipole only



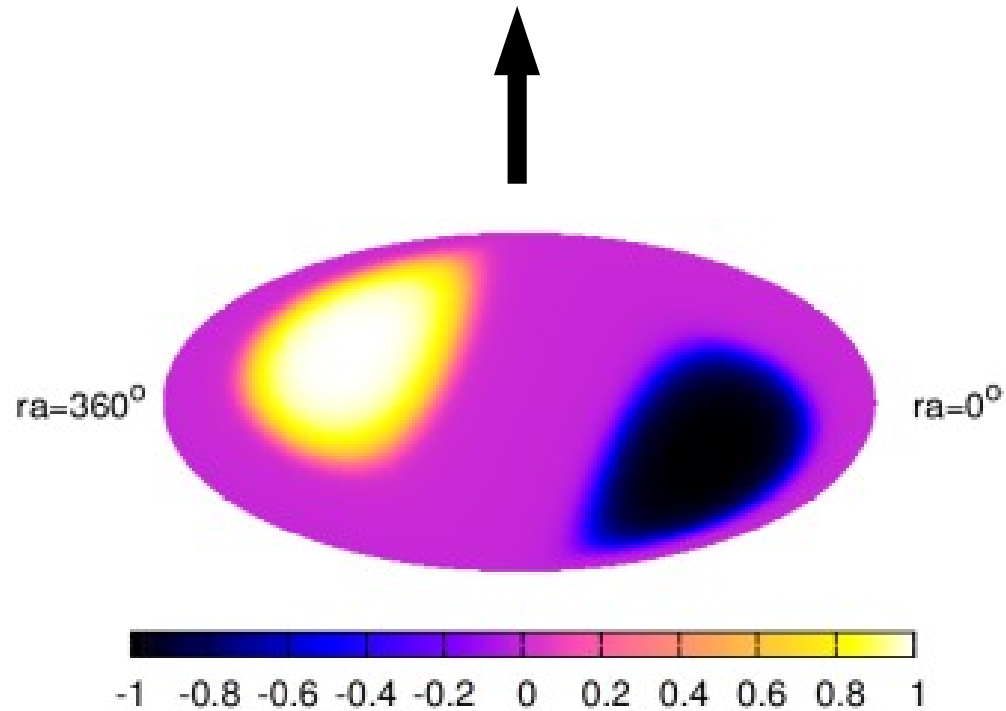
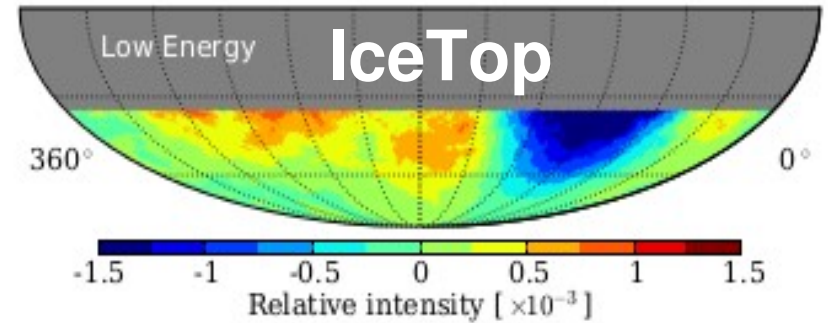
Or could the L-S CR anisotropy look like this ? :



Cosmic-Ray Anisotropy

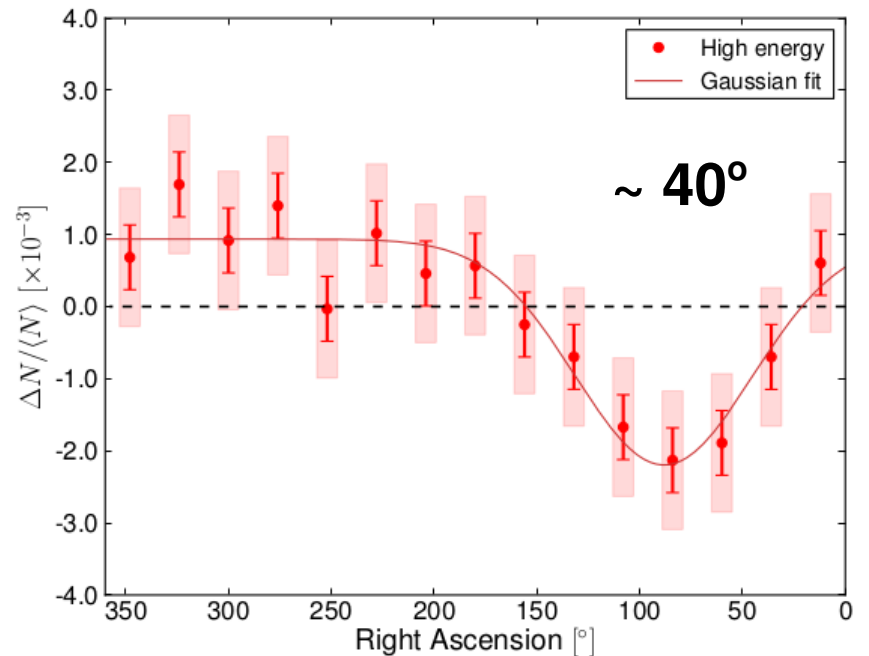
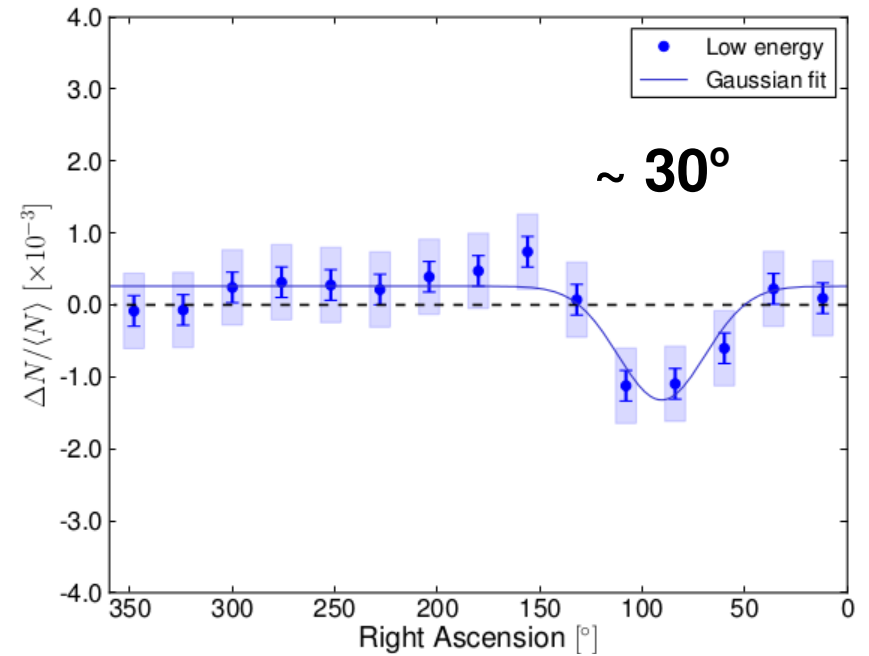
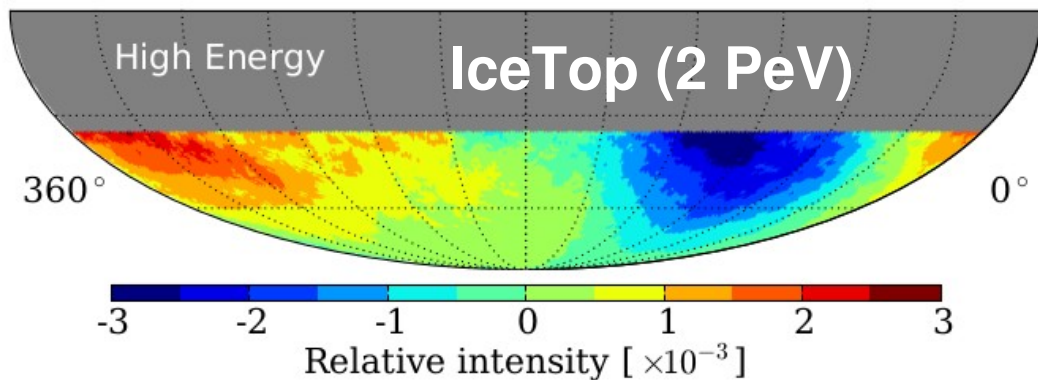
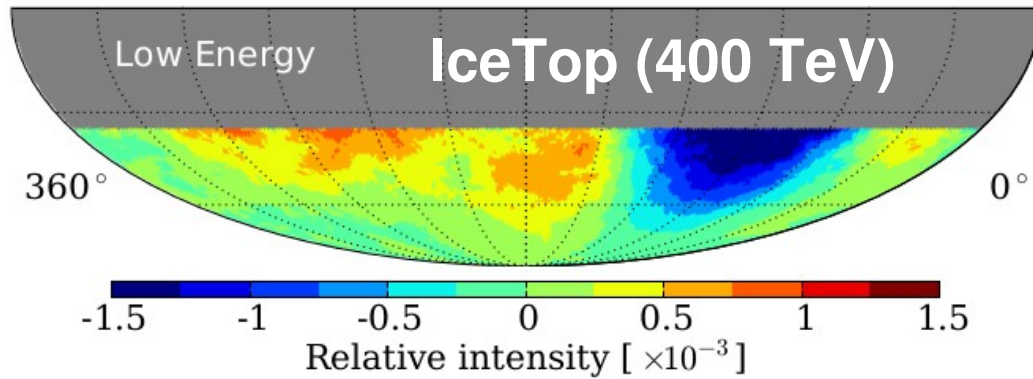


vs



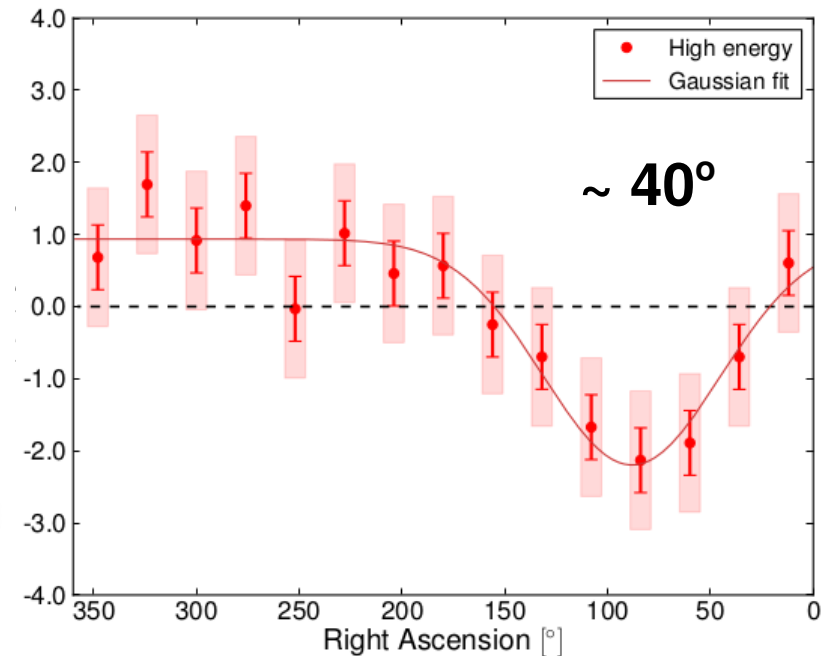
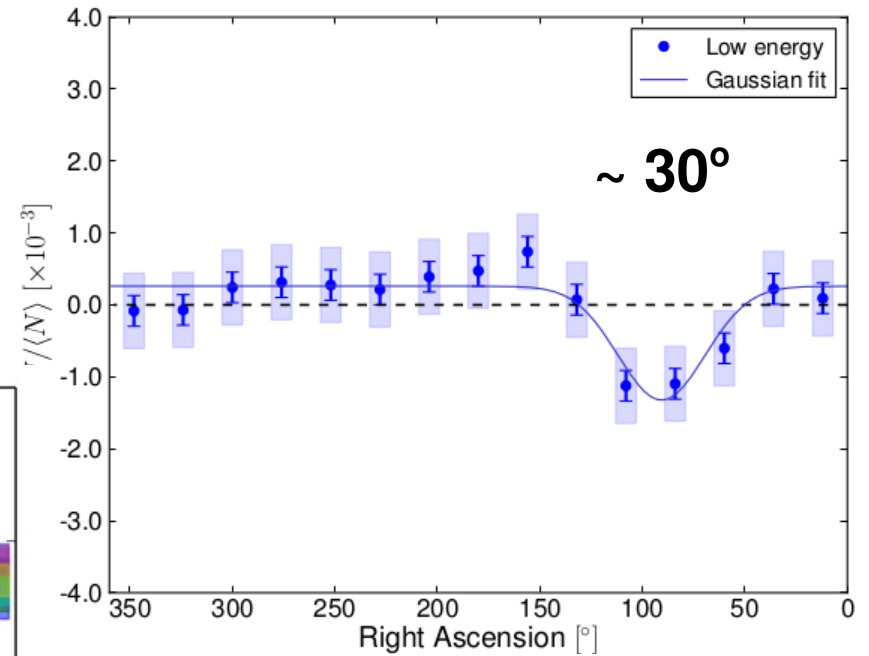
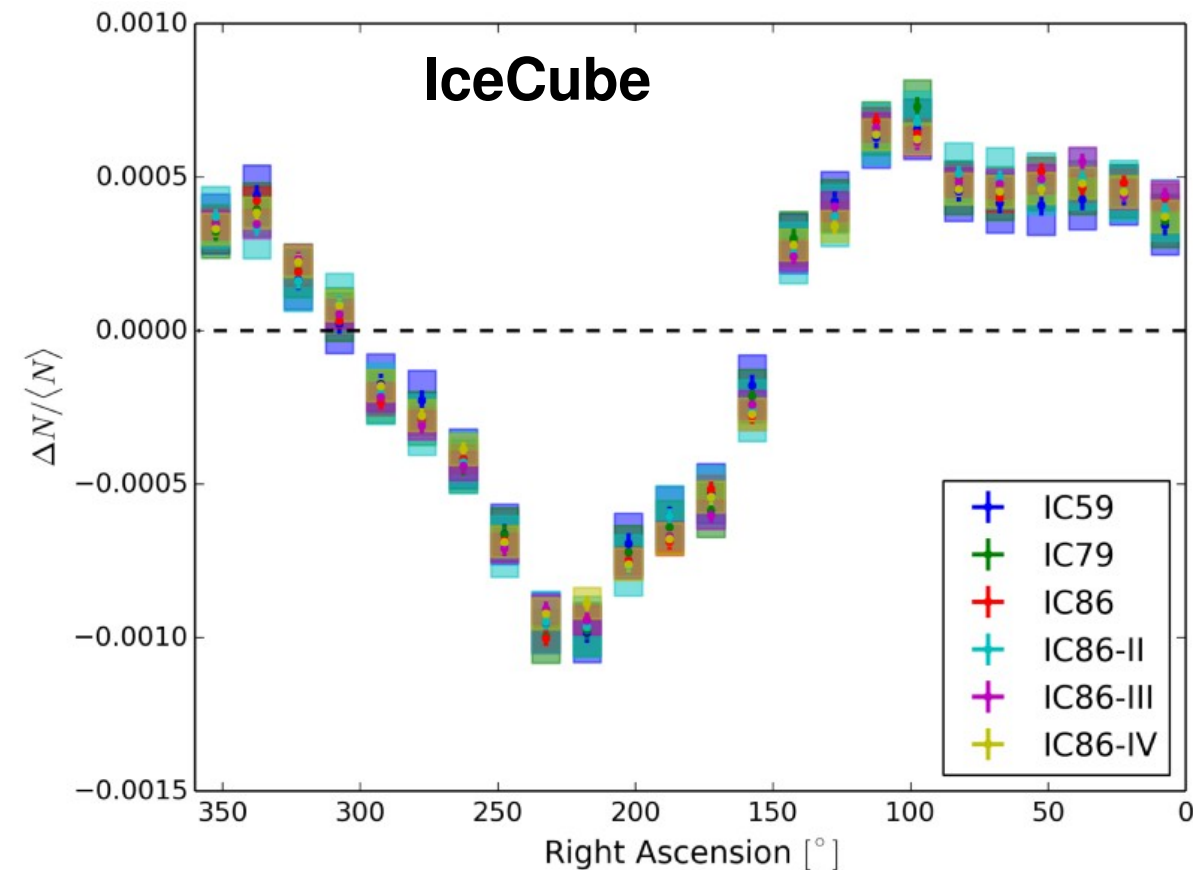
Observations (IceCube, IceTop)

Aartsen et al. (2013)



Observations (IceCube, IceTop)

Aartsen et al. (2016)



Local MF lines and L-S CR Anisotropy

Global Anisotropies in TeV Cosmic Rays Related to the Sun's Local Galactic Environment from IBEX

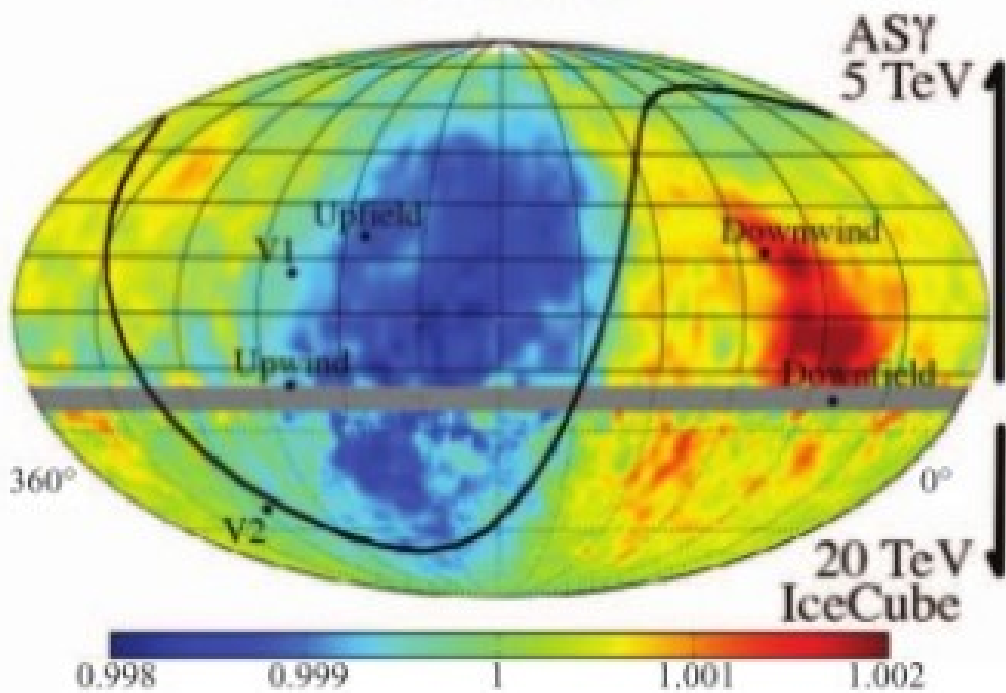
N. A. Schwadron *et al.*

Science **343**, 988 (2014);

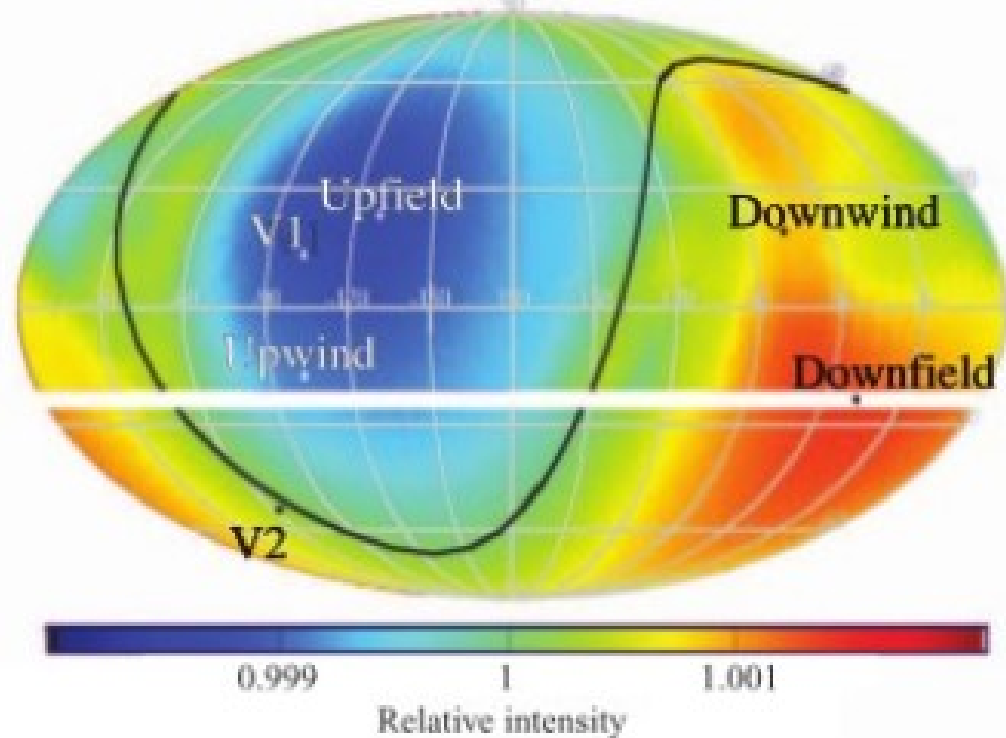
Frisch et al. 2012

→ *local field*

Observed

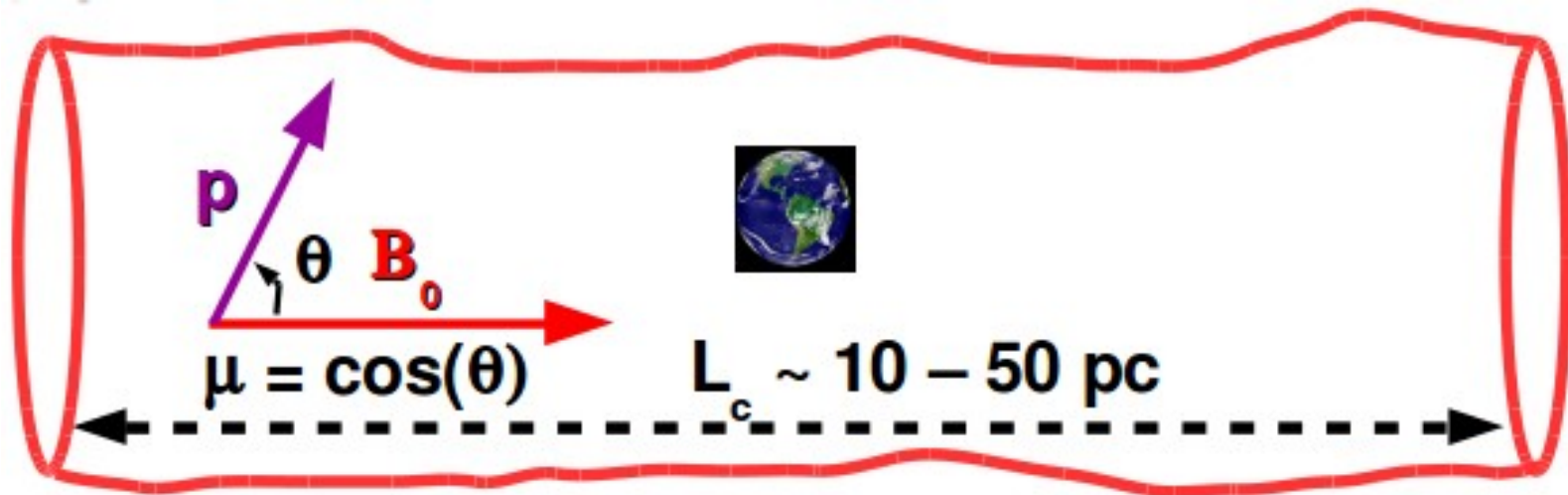


Interstellar Conditions from IBEX



... and $\delta B/B_0 \ll 1$

CR Anisotropy : Probe of turbulence



$$\mu v \frac{\partial f}{\partial x} = \frac{\partial}{\partial \mu} \left(D_{\mu\mu} \frac{\partial f}{\partial \mu} \right)$$

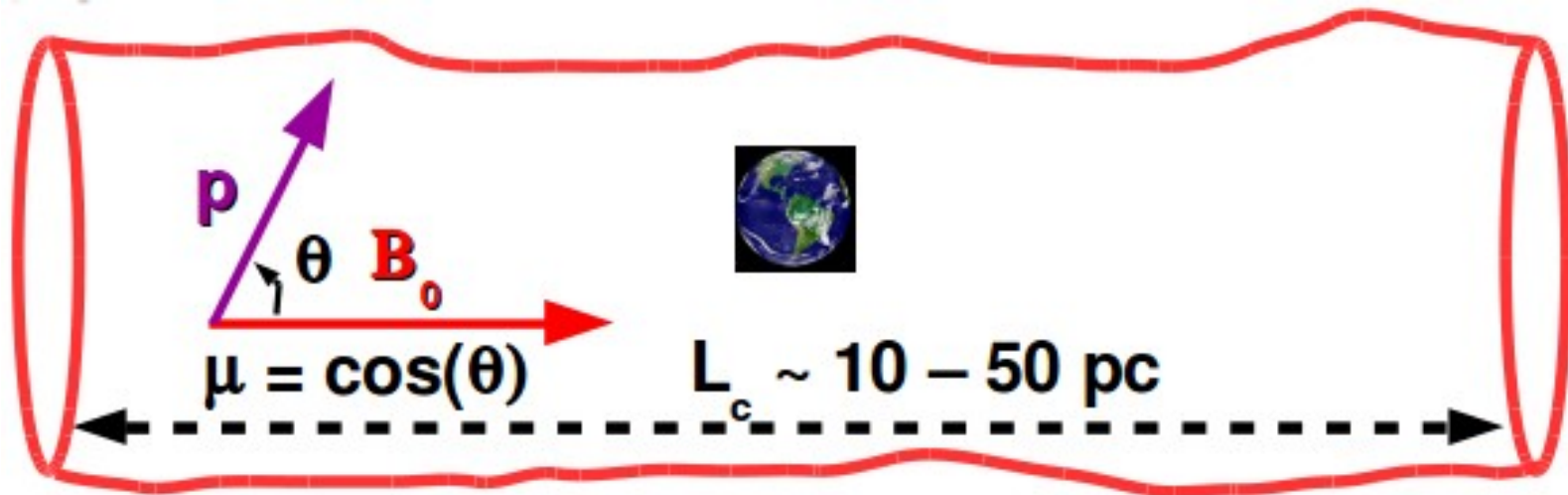
(gyrophase-averaged)

$$\Rightarrow f(x, \mu) = \sum_i a_i e^{\Lambda_i x/v} Q_i(\mu) + a_{\text{diff}} [x + g(\mu)]$$

if $\exp(-\Lambda_1 d/v) \ll 1$

(« boundary layer »)

CR Anisotropy : Probe of turbulence



NOT $1 - \mu^2$ in general \Rightarrow NOT a dipole!

$$\int_0^\mu d\mu' \frac{1 - \mu'^2}{D_{\mu'\mu'}}$$

$$\Rightarrow f(x, \mu) = \sum_i a_i e^{\Lambda_i x/v} Q_i(\mu) + a_{\text{diff}} [x + g(\mu)]^\alpha$$

if $\exp(-\Lambda_1 d/v) \ll 1$

(« boundary layer »)

Pitch-angle diffusion coefficient

$$D_{\mu\mu} = \Omega^2 (1 - \mu^2) \int d^3k \int_0^\infty d\tau \sum_{n=-\infty}^{\infty} \left(\frac{n^2 J_n^2(z)}{z^2} M_A(\mathbf{k}, \tau) + \frac{k_{\parallel}^2 J_n'^2(z)}{k^2} M_{S,F}(\mathbf{k}, \tau) \right),$$

where $z = k_{\perp} l \varepsilon \sqrt{1 - \mu^2}$, and Ω is the Larmor frequency. $M_{A,S,F}$ respectively represent the normalized power spectra of Alfvén, slow and fast modes:

$$\varepsilon = v / (l\Omega) = r_L / l$$

$$M_w(\mathbf{k}, \tau) = \langle \mathbf{B}_{1,w}(\mathbf{k}, t) \cdot \mathbf{B}_{1,w}^*(\mathbf{k}, t + \tau) \rangle / B_0^2,$$

$$\Rightarrow D_{\mu\mu} = \Omega^2 (1 - \mu^2) \int d^3k \sum_{n=-\infty}^{\infty} \left(\frac{n^2 J_n^2(z)}{z^2} \mathcal{I}_A(\mathbf{k}) + \frac{k_{\parallel}^2 J_n'^2(z)}{k^2} \mathcal{I}_{S,F}(\mathbf{k}) \right) \times R_n(k_{\parallel} v_{\parallel} - \omega + n\Omega),$$

where $\mathcal{I}_{A,S,F}$ respectively correspond to the normalized energy spectra of the Alfvén, slow and fast modes.

Resonance functions

RF dominated by Lagrangian correlation time :

« **NARROW** »

$$\underline{R_{n,1}(k_{\parallel} v_{\parallel} - \omega + n\Omega)}$$

$$= \text{Re} \left(\int_0^{\infty} d\tau e^{-i(k_{\parallel} v_{\parallel} - \omega + n\Omega)\tau - \tau/\tau_w} \right)$$

see Chandran (2000)

$$= \frac{\tau_w^{-1}}{(k_{\parallel} v_{\parallel} - \omega + n\Omega)^2 + \tau_w^{-2}}$$

$$\tau_{A,S} = l^{1/3} / (v_A k_{\perp}^{2/3})$$

$$\tau_F = l / (v_A \tilde{k}^{1/2}) \quad \tilde{k} = kl$$

Conservation of the adiabatic invariant v_{\perp}^2 / B

« **BROAD** »

The variations of v_{\parallel} are dominated by the variations δB_{\parallel}

$$\underline{R_{n,2}(k_{\parallel} v_{\parallel} - \omega + n\Omega)}$$

$$= \text{Re} \left(\int_0^{\infty} d\tau e^{-i(k_{\parallel} v_{\parallel} - \omega + n\Omega)\tau - k_{\parallel}^2 v_{\perp}^2 \delta \mathcal{M}_A \tau^2 / 2} \right)$$



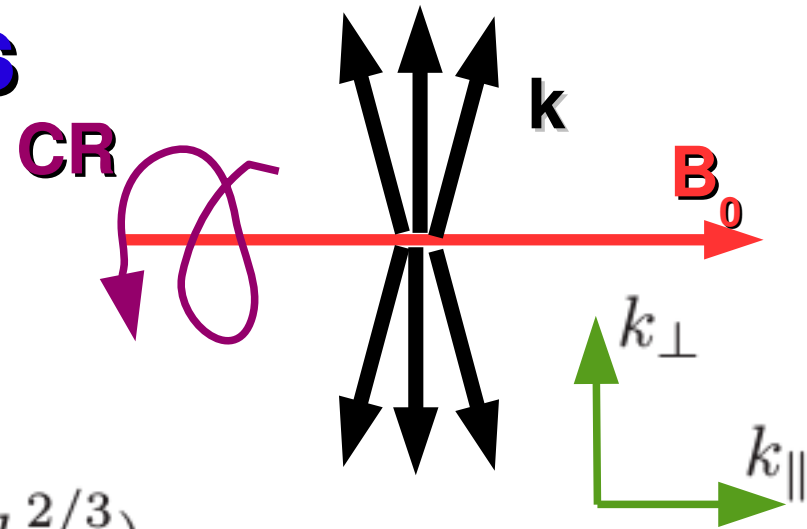
$$= \frac{\sqrt{\pi}}{k_{\parallel} v_{\perp} \delta \mathcal{M}_A^{1/2}} \exp \left(- \frac{(k_{\parallel} v_{\parallel} - \omega + n\Omega)^2}{k_{\parallel}^2 v_{\perp}^2 \delta \mathcal{M}_A} \right)$$

$$\delta \mathcal{M}_A = \sqrt{\langle \delta B_{\parallel}^2 \rangle} / B_0^2$$

Alfven (and Slow) modes

Goldreich & Sridhar (1995)

$$|k_{\parallel}| \lesssim |k_{\perp}|^{2/3} l^{-1/3}$$



(1) $\mathcal{I}_{A,S} = \mathcal{I}_{1,A,S} \propto k_{\perp}^{-10/3} h(k_{\parallel} l^{1/3} / k_{\perp}^{2/3})$

where $h(y) = 1$ if $|y| < 1$, and $h = 0$ otherwise (see Chandran (2000))

(2) MHD simulations of Cho & Lazarian (2002) :

$$\mathcal{I}_{A,S} = \mathcal{I}_{2,A,S} \propto k_{\perp}^{-10/3} \exp(-k_{\parallel} l^{1/3} / k_{\perp}^{2/3})$$

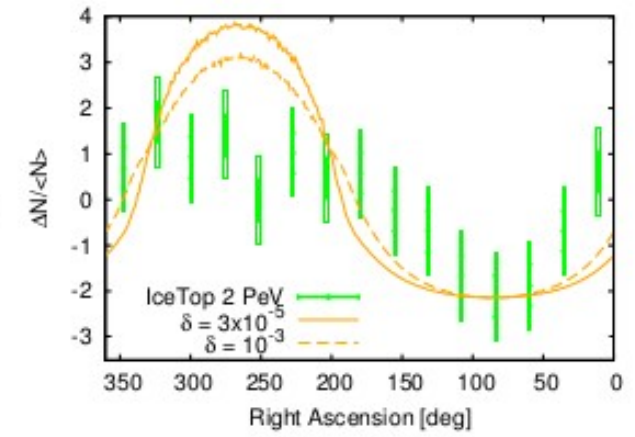
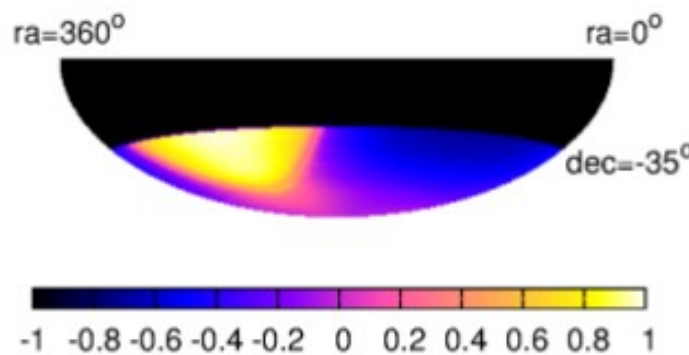
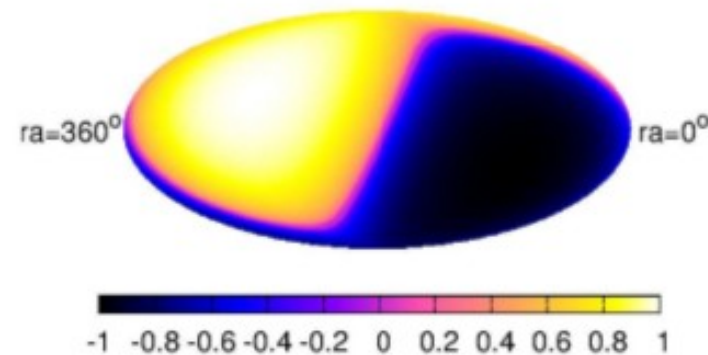
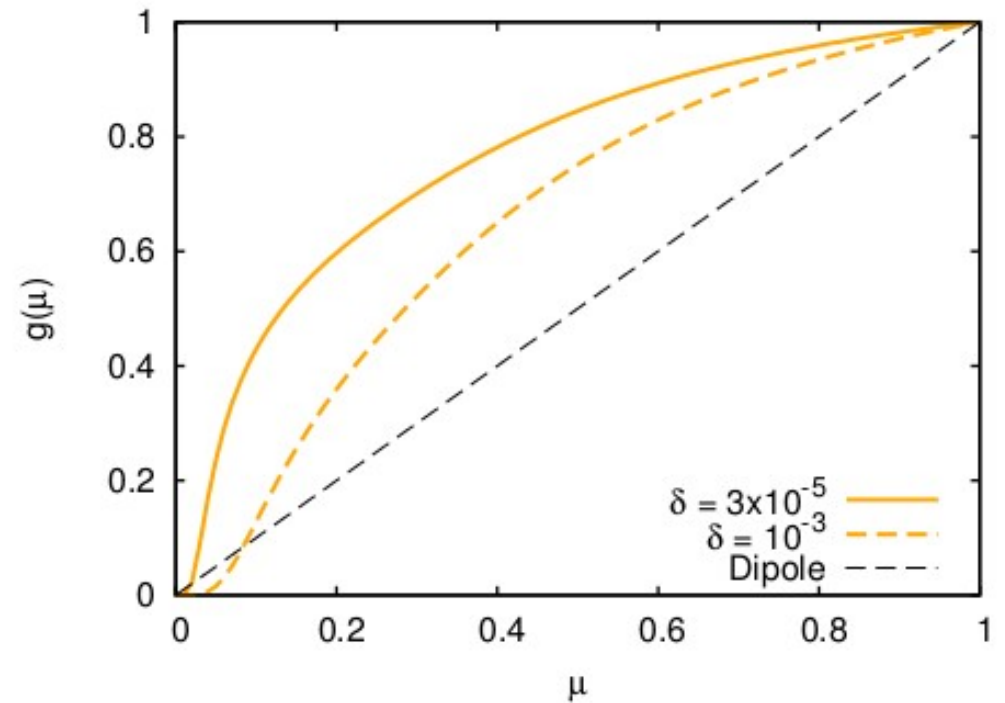
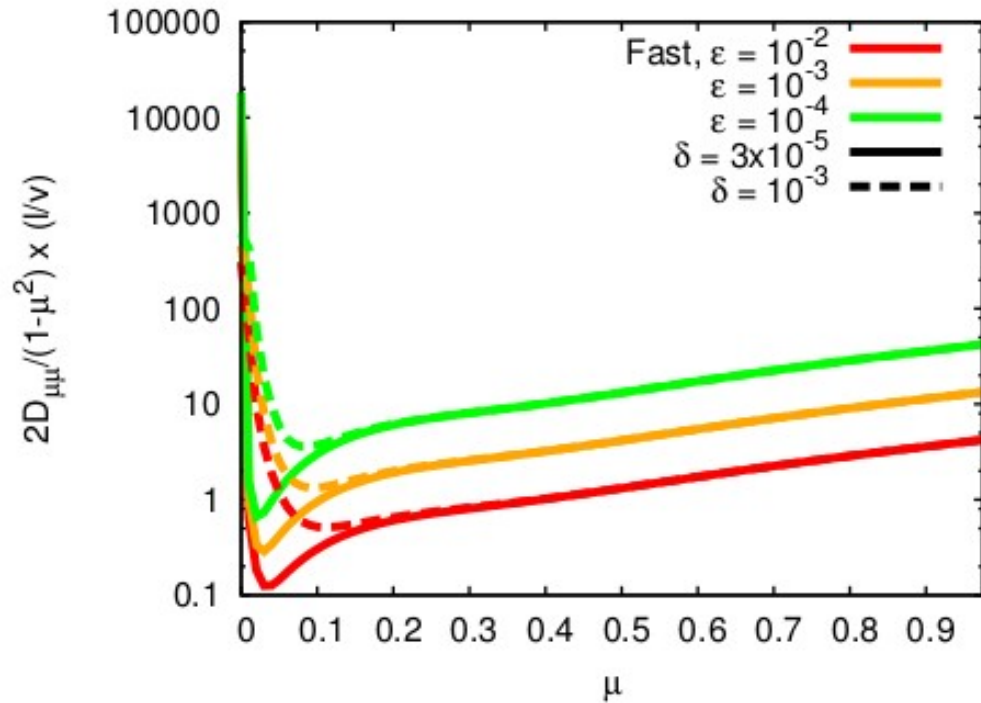
Fast magnetosonic modes

MHD simulations of Cho & Lazarian (2002) :

$$\text{Isotropic with } \mathcal{I}_M(\mathbf{k}) \propto k^{-3/2}$$

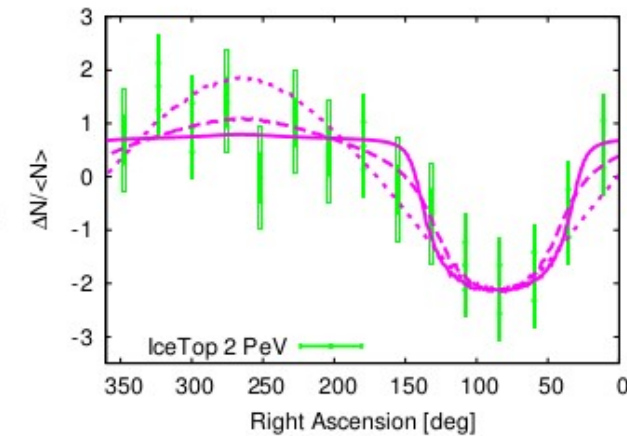
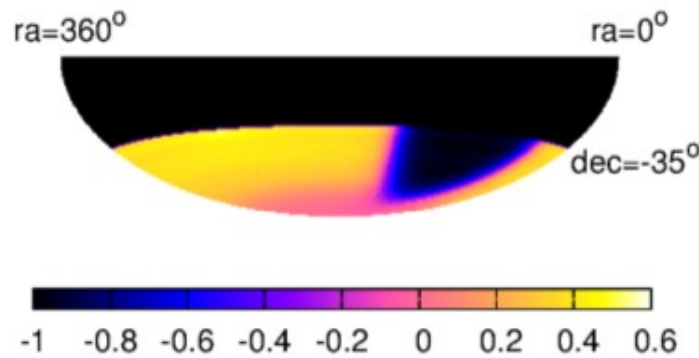
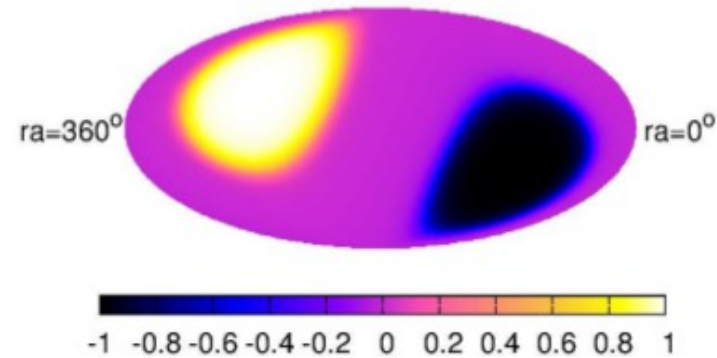
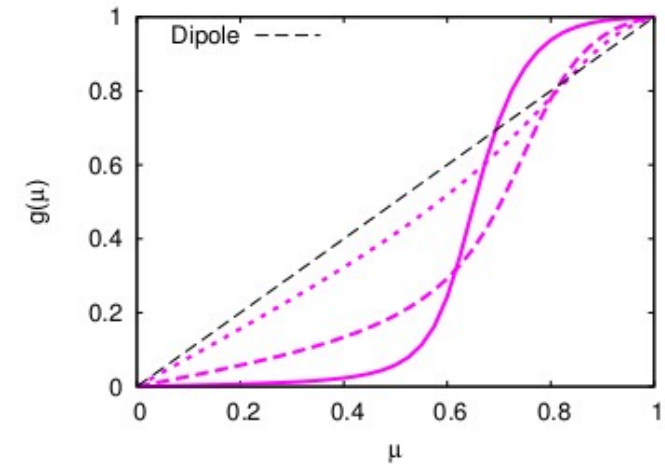
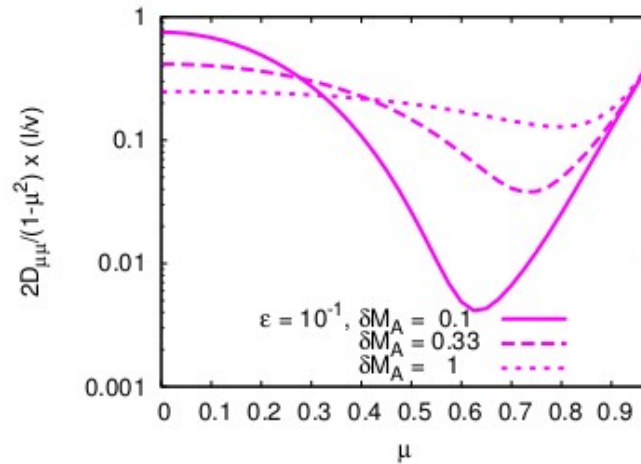
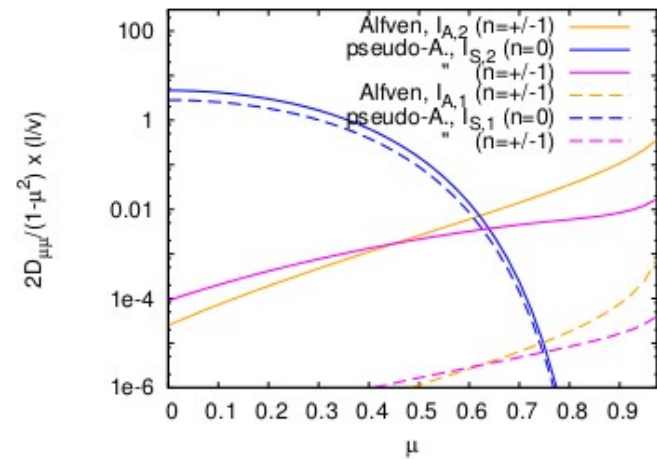
Fast modes ('Narrow' RF)

No visible dependence of the *shape* on CR energy

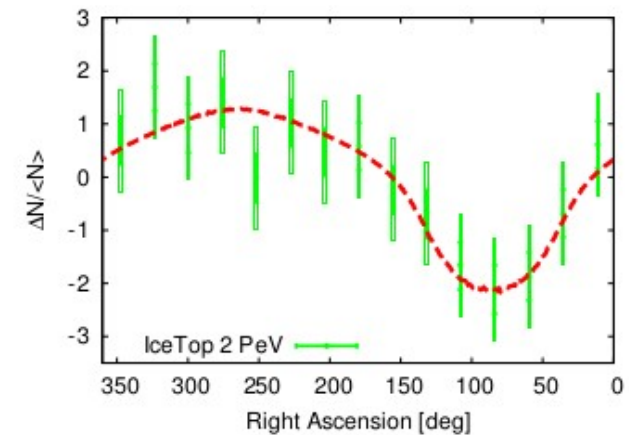
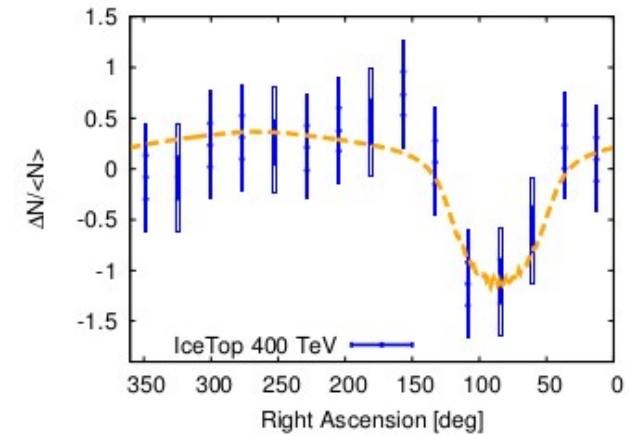
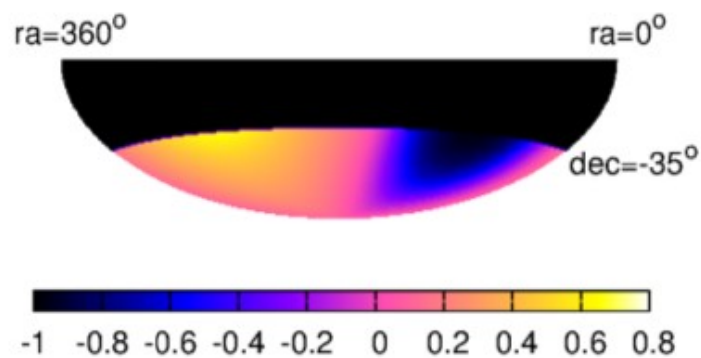
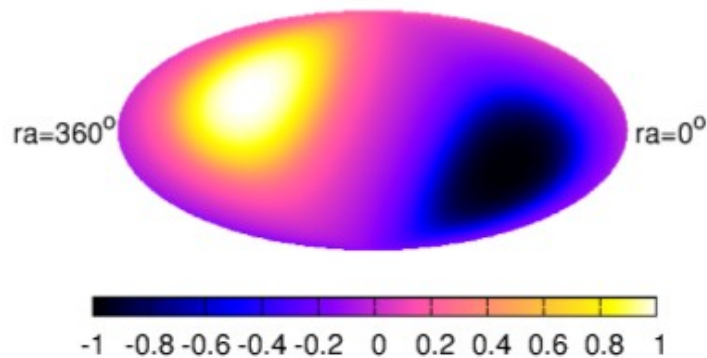
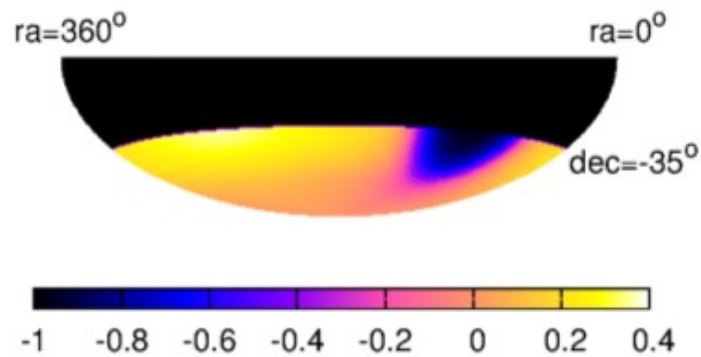
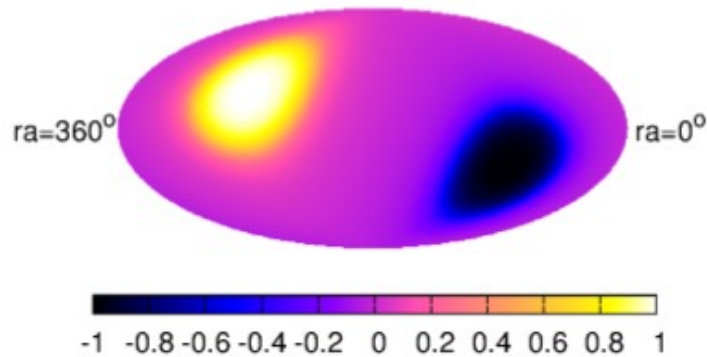


RULED OUT !

GS ('Heaviside', 'Broad' RF)



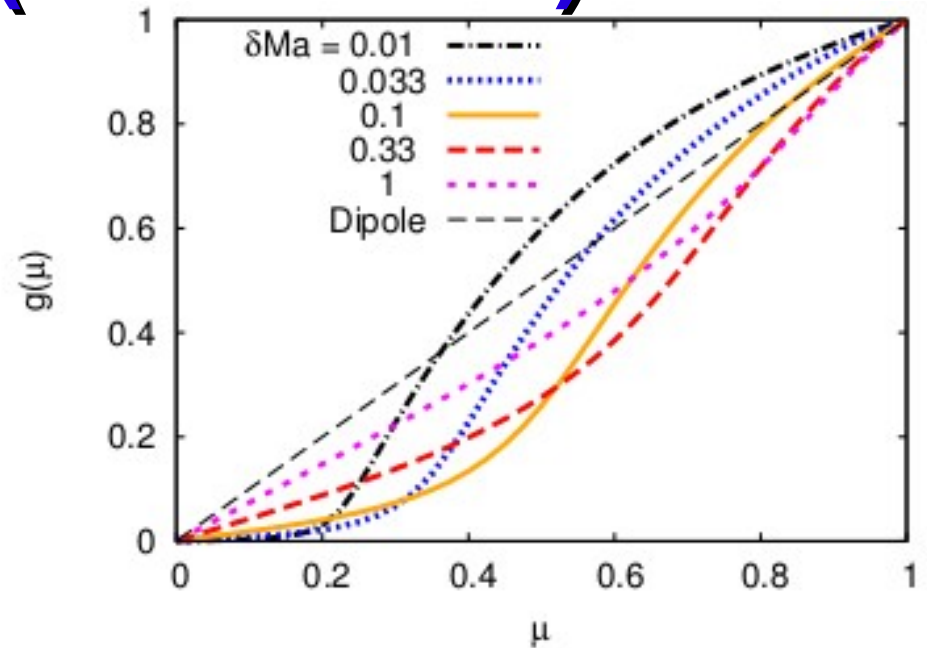
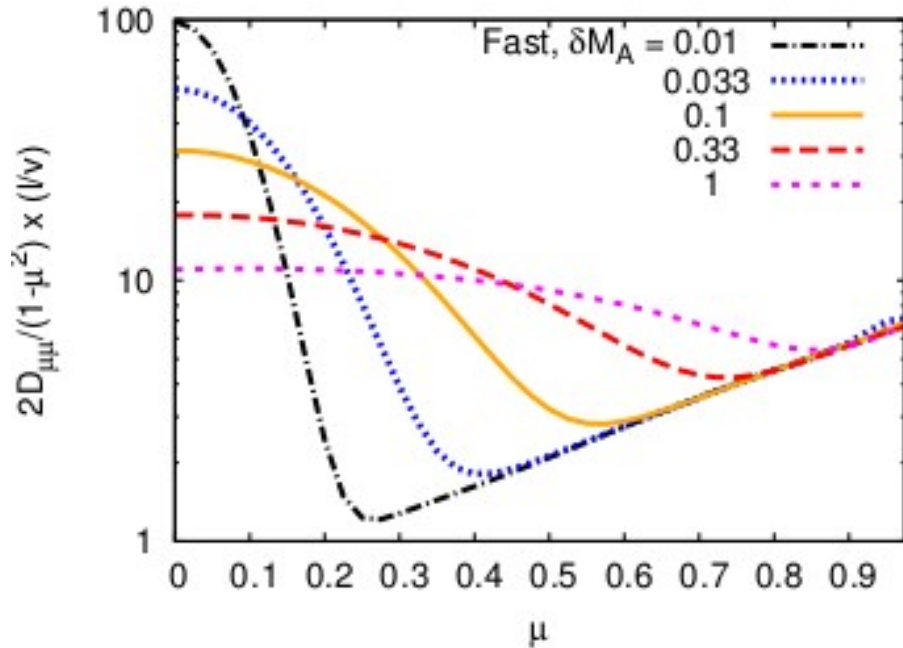
GS ('Exponential', 'Broad' RF)



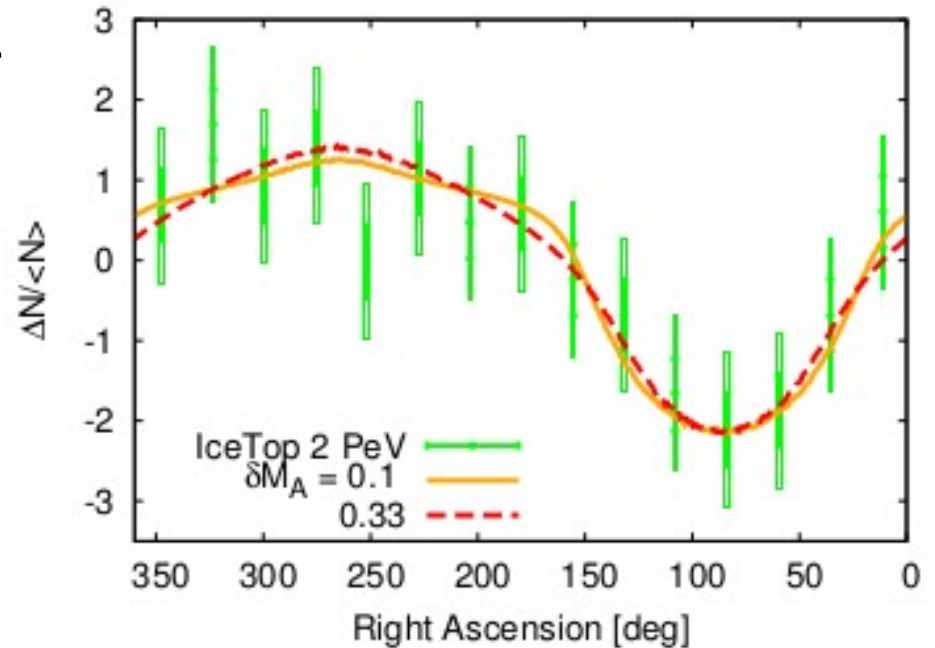
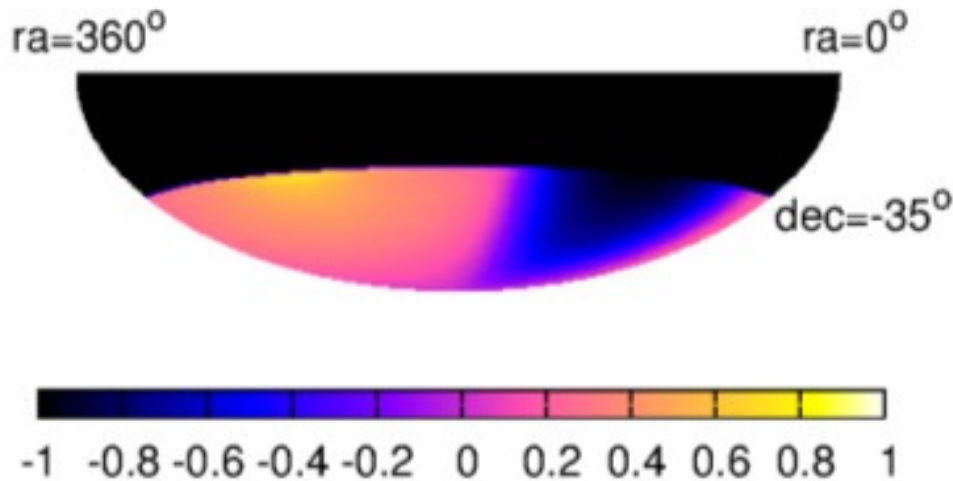
Can fit well the 400 TeV and the 2 PeV data !

Energy-dependence reproduced for fixed turbulence parameters

Fast modes ('Broad' RF)



No dependence of the *shape* on E
Can fit well the 2 PeV data !



Conclusions and perspectives

- Flattening in directions perpendicular to field lines
- Can fit the 2 PeV data with GS turbulence or fast modes
- Change in anisotropy shape with CR energy ?
- Constraints on resonance functions

Large-scale CR Anisotropy : New probe of

(1) local ISMFs (Modes and their anisotropy in k-space)

Probe of turbulence in collisionless magnetized fluids

(2) local CR transport properties